



JRC TECHNICAL REPORT

Extreme and long-term drought in the La Plata Basin: event evolution and impact assessment until September 2022

*A joint report EC-JRC,
CEMADEN, CIMA, SISSA, and
WMO*

Naumann, G., Podestá, G., Marengo, J.,
Luterbacher, J., Bavera D., Acosta Navarro, J.,
Arias Muñoz, C., Barbosa, P., Cammalleri, C.,
Cuartas, A., de Estrada, M., de Felice M., de
Jager, A., Escobar, C., Fioravanti, G., Giordano,
L., Harst Essenfelder, A., Hidalgo, C., Leal de
Moraes, O., Maetens, W., Magni, D., Masante,
D., Mazzeschi, Osman, M., Rossi L., M., Seluchi,
M., Skansi, M. M., Spennemann, P., Spinoni, J.,
Toreti., A, Vera, C.

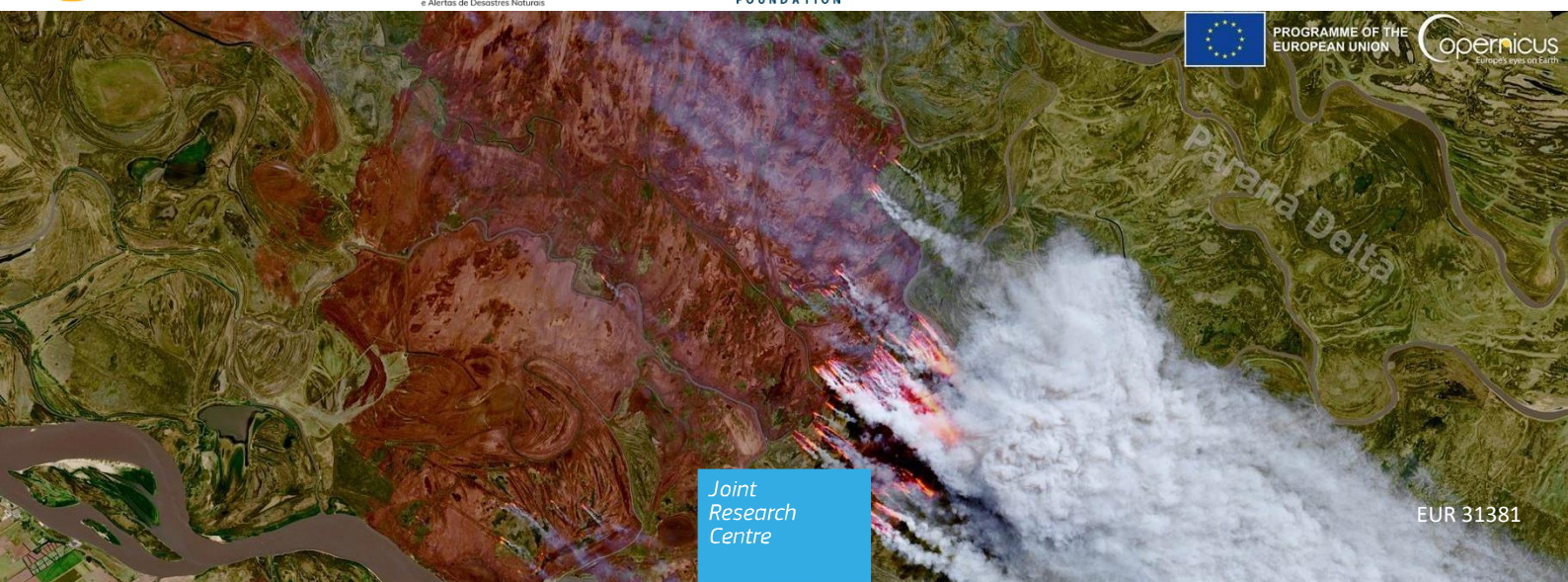
2023



WORLD
METEOROLOGICAL
ORGANIZATION



PROGRAMME OF THE
EUROPEAN UNION



Joint
Research
Centre

EUR 31381

This publication is a Technical report by the Joint Research Centre (JRC), the European Commission's science and knowledge service. It aims to provide evidence-based scientific support to the European policymaking process. The contents of this publication do not necessarily reflect the position or opinion of the European Commission. Neither the European Commission nor any person acting on behalf of the Commission is responsible for the use that might be made of this publication. For information on the methodology and quality underlying the data used in this publication for which the source is neither Eurostat nor other Commission services, users should contact the referenced source. The designations employed and the presentation of material on the maps do not imply the expression of any opinion whatsoever on the part of the European Union concerning the legal status of any country, territory, city or area or of its authorities, or concerning the delimitation of its frontiers or boundaries.

Contact information

Name: Andrea Toreti

Address: Via E. Fermi 2749, I-21027 ISPRA (VA), Italy

Email: Andrea.TORETI@ec.europa.eu

EU Science Hub

<https://joint-research-centre.ec.europa.eu>

JRC132245

EUR 31381 EN

PDF ISBN 978-92-76-61614-6 ISSN 1831-9424 [doi:10.2760/62557](https://doi.org/10.2760/62557) KJ-NA-31-381-EN-N

Luxembourg: Publications Office of the European Union, 2023

© European Union, 2023



The reuse policy of the European Commission documents is implemented by the Commission Decision 2011/833/EU of 12 December 2011 on the reuse of Commission documents (OJ L 330, 14.12.2011, p. 39). Unless otherwise noted, the reuse of this document is authorised under the Creative Commons Attribution 4.0 International (CC BY 4.0) licence (<https://creativecommons.org/licenses/by/4.0/>). This means that reuse is allowed provided appropriate credit is given and any changes are indicated. For any use or reproduction of photos or other material that is not owned by the European Union permission must be sought directly from the copyright holders. The European Union does not own the copyright in relation to the following elements:

- page 10, Figure 3, source: SISSA
- page 11, Figure 4, source: SISSA
- page 16, Figure 10, source: Instituto Nacional del Agua, Argentina
- page 17, Figure 11, source: CEMADEN
- page 18, Figure 12, source: Adapted from Spennemann et al., 2022
- page 21, Figure 14, source: WMO-KNMI climate explorer <https://climexp.knmi.nl>
- page 22, Figure 15, source: WMO-KNMI climate explorer <https://climexp.knmi.nl>
- page 24, Figure 16, source: Copernicus Climate Change Service
- page 24, Figure 17, source: NOAA, CPC
- page 25, Figure 18, source: APEC Climate Center
- page 26, Figure 19, source: WMO-KNMI climate explorer <https://climexp.knmi.nl>
- page 27, Figure 20, source: <https://hadleyserver.metoffice.gov.uk/wmolc/>
- page 29, Figure 21, source: SISSA
- page 30, Figure 22, source: SISSA
- page 31, Figure 23, source: INTA Corrientes
- page 34, Figure 25, source: CEMADEN
- page 35, Figure 26, source: Instituto Nacional del Agua, Argentina
- page 37, Figure 27, source: websites of the national transmission system operators for countries shown:
- page 38, Figure 28, source: Mesa Nacional de Monitoreo de Sequías, Argentina
- page 39, Figure 29, source: <https://monitordesecas.ana.gov.br>
- page 40, Figure 30, source: CEMADEN
- page 41, Figure 31, source: CEMADEN
- page 42, Figure 32, source: CEMADEN
- page 43, Figure 33, source: Bolivian Drought Monitor (<http://monitoresequias.senamhi.gob.bo>)
- page 44, Figure 34, source: INUMET and INIA/GRAS

Cover page illustration: Several wildfires are devastating the wetlands of the second-longest river in South America, the Paraná. The blazes have ignited in northern Argentina, close to the city of Rosario, following a prolonged period of drought and scarce rainfall. Nearly 100,000 hectares of land have burnt in the past two weeks, threatening the wetland ecosystems and heavily affecting air quality. The smoke from the fires has in fact reached the city of Buenos Aires, almost 300 km south of the hotspots. This image, acquired on 19 August 2022, shows a large active fire burning near Villa Constitución, southeast of Rosario. © European Union, Copernicus Sentinel-2 imagery

How to cite this report: Naumann, G., Podestá, G., Marengo, J., Luterbacher, J., Bavera D., Acosta Navarro, J., Arias Muñoz, C., Barbosa, P., Cammalleri, C., Cuartas, A., de Estrada, M., de Felice M., de Jager, A., Escobar, C., Fioravanti, G., Giordano, Harst Essenfelder, A., L., Hidalgo, C., Leal de Moraes, O., Maetens, W., Magni, D., Masante, D., Mazzeschi, Osman, M., Rossi L., M., Seluchi, M., Skansi, M. M., Spennemann, P., Spinoni, J., Toreti, A., Vera, C., *Extreme and long-term drought in the La Plata Basin: event evolution and impact assessment until September 2022*, Publications Office of the European Union, Luxembourg, 2022, doi:10.2760/62557, JRC132245.

Contents

Abstract.....	3
Acknowledgements.....	4
1 Introduction.....	6
2 Evolution and status of the 2019-present drought in the La Plata Basin	8
2.1 Standardized Precipitation Index (SPI).....	8
2.2 Spatial evolution of areas under different drought categories based on CHIRPS precipitation estimates 9	
2.3 Hydrological variables	11
2.4 Vegetation response	13
2.5 Streamflow indicators of drought conditions	15
2.5.1 Paraná River streamflow at Corrientes, Argentina	15
2.5.2 Streamflow at Emborcação, Furnas, Jurumirim, Foz do Areia and Itaipu hydro-power plants in the Upper Paraná River.....	16
2.6 Monitoring drought using combined indicators: the JRC Combined Drought Index	17
2.7 Summary of drought conditions	18
3 Associated circulation patterns and seasonal and decadal outlooks	20
3.1 Seasonal prediction and outlook	20
3.2 Decadal prediction	26
4 Reported impacts of the present drought.....	28
4.1 Ecosystems – Wetlands.....	28
4.2 Fires.....	28
4.3 Crops, Livestock and Economy.....	32
4.4 Waterway Transportation.....	33
4.5 Hydroelectricity generation and other energy impacts and water supply for human consumption	36
5 Knowing and doing better: ongoing efforts on regional drought monitoring.....	38
5.1 Drought monitoring in Argentina.....	38
5.2 Drought Monitoring in Brazil	39
5.2.1 Drought Monitor of the National Water Agency	39
5.2.2 Drought Monitoring System of CEMADEN	40
5.3 Drought monitoring in Bolivia	42
5.4 Drought monitoring in Paraguay.....	43
5.5 Drought monitoring in Uruguay.....	43
5.6 Regional drought monitoring: Sistema de Información sobre Sequías para el sur de Sudamérica - SISSA 44	
6 Conclusions.....	45
References	46
List of abbreviations and definitions	49

List of figures	50
List of tables	53
Annexes.....	54
Annex 1. Description of drought indicators used in this report	54

Abstract

The current drought conditions across the Parana-La Plata Basin (LPB) in Brazil-Argentina have been the worst since 1944. While this area is characterized by a rainy season with a peak from October to April, the hydrological year 2020-2021 was very deficient in rainfall, and the situation extended into the 2021-2022 hydrological year. Below-normal rainfall was dominant in south-eastern Brazil, northern Argentina, Paraguay, and Uruguay, suggesting a late onset and weaker South American Monsoon and the continuation of drier conditions since 2021. In fact, in 2021 Brazilian south and south-east regions faced their worst droughts in nine decades, raising the spectre of possible power rationing given the grid dependence on hydroelectric plants. The Paraná-La Plata Basin drought induced damages to agriculture and reduced crop production, including soybeans and maize, with effects on global crop markets. The drought situation continued in 2022 in the Pantanal region.

Dry meteorological conditions are still present in the region at the end of September 2022 with below-average precipitation anomalies. Soil moisture anomaly and vegetation conditions are worst in the lower part of the La Plata Basin. Conversely, the upper and central parts of the basin show partial and temporary recovery.

Seasonal modelling systems consistently forecast negative precipitation anomalies over the LPB as a response to the negative sea surface temperatures (SST) anomalies in the tropical Pacific associated with La Niña condition. There are high chances that La Niña conditions will prevail for the third spring and summer in a row (last time was during 1998-2001). Similarly, multi-annual to decadal modes of climate variability (i.e., AMO, PDO) have been in a phase that favours drought in the LPB in the period 2019/2020-present.

Acknowledgements

Research at “Centro Nacional de Monitoramento e Alertas de Desastres Naturais” (CEMADEN) was partly funded by the INCT-Climate Change Phase 2 project (Conselho Nacional de Desenvolvimento Científico e Tecnológico, Grant/Award Number: 465501/2014-1; Coordenação de Aperfeiçoamento de Pessoal de Nível Superior, Grant/Award Number: 88887.136402/2017-; Fundação de Amparo à Pesquisa do Estado de São Paulo, Grant/Award Number: 2014/50848-9; CNPq, Grant/Award Number: 301397/2019-8).

The “Sistema de Información sobre Sequías para el Sur de Sudamérica” (SISSA) is a component of the Regional Climate Centre for southern South America, a six-nation collaboration to produce and disseminate timely, relevant, and actionable climate information and services to support decision-making in societal sectors sensitive to climate variability and change. Main support for SISSA activities is provided by the Regional Public Goods program of the Inter-American Development Bank and by the Euroclima+ program funded by the European Union through the Spanish Agency for International Development.

Authors

Gustavo Naumann, CIMA Research Foundation, Italy

Guillermo Podestá, SISSA, Argentina

Jose Antonio Marengo, CEMADEN, Brazil

Jürg Luterbacher, Director Science and Innovation Department and Chief Scientist, World Meteorological Organization, Switzerland

Davide Bavera, Arcadia SIT, Italy

Juan Camilo Acosta Navarro, European Commission, Joint Research Centre, Italy

Carolina Arias Muñoz, Arhs Development, Italy

Paulo Barbosa, European Commission, Joint Research Centre, Italy

Carmelo Cammalleri, European Commission, Joint Research Centre, Italy.

Luz Adriana Cuartas, CEMADEN, Brazil

María de Estrada, Ministerio de Agricultura, Ganadería y Pesca, Argentina

Matteo de Felice, European Commission, Joint Research Centre, Italy

Alfred de Jager, European Commission, Joint Research Centre, Italy

Cristián Escobar, World Meteorological Organization, Regional Office for South America, Paraguay

Guido Fioravanti, European Commission, Joint Research Centre, Italy

Leandro Giordano, Instituto Nacional del Agua, Argentina

Arthur Hraст Essenfelder, European Commission, Joint Research Centre, Italy

Cecilia Hidalgo, SISSA, Universidad de Buenos Aires, Argentina

Osvaldo Luiz Leal de Moraes, CEMADEN, Brazil

Willem Maetens, European Commission, Joint Research Centre, Italy

Diego Magni, Arcadia SIT, Italy

Dario Masante, European Commission, Joint Research Centre, Italy

Marco Mazzeschi, Uni Systems Luxembourg Srl, Luxembourg

Marisol Osman, Karlsruhe Institute of Technology, Germany

Lauro Rossi, CIMA Research Foundation, Italy

Marcelo Enrique Seluchi, CEMADEN, Brazil

Maria de los Milagros Skansi, National Weather Service, Argentina

Pablo Spennemann CONICET-National Weather Service, Argentina

Jonathan Spinoni, European Commission, Joint Research Centre, Italy

Andrea Toreti, European Commission, Joint Research Centre, Italy

Carolina Vera, SISSA, Argentina

1 Introduction

In the past two years, the Paraná River, the second-longest in South America and traversing Paraguay, Argentina, and Brazil⁽¹⁾, has been experiencing its lowest water levels in 77 years (Naumann et al., 2021). In 2021, the Rio Paraná flow rate significantly reduced from an average of 17,000 to 6,200 cubic meters per second. The deficit is well visible in the image acquired by the Copernicus Sentinel-2 on 27 November 2021, showing the low flows in the Paraná River near Corrientes in Argentina (Figure 1). At the time of image acquisition, the level of the Paraná River in Corrientes was 2.64 meters below the monthly November average (based on the last 25 years).

This decrease can partially be attributed to the La Niña event that started in 2020 and has been extending into 2022 (WMO, 2022). Yet, other factors such as land-use change and the occurrence of extreme events also play a role in the flow rate reduction of the Parana River. In 2020, a summer drought combined with a heatwave affected central South America contributing to the increase of fires in the region (Marengo et al., 2021; Marengo, Cunha, et al., 2021). This situation repeated in 2021, where drought conditions continued and heatwaves were reported in west, central and south-eastern Brazil, including the Pantanal region even though with lower intensity (Libonati et al., 2022).

Over the last decade, Brazil has experienced the worst droughts in the available observational records with severe socioeconomic and environmental impacts. Cuartas et al., (2022) shows that since the 2014-15 drought over southeast Brazil, several basins (that were strongly affected) have not fully recovered yet, and some are still dealing with on-going critical conditions. Following the 2014-15 drought event, other regions have experienced droughts with critical rainfall deficit together with high temperatures, causing pronounced impacts on water availability in many of the studied basins. Most of the hydropower plants ended the 2020–2021 rainy season by operating at a fraction of their total capacity, and thus Brazilian hydropower generation was under critical conditions (Cuartas et al., 2022). Despite some months with above-normal rainfall in 2016 and 2017 (mainly in the form of short heavy precipitation events), reservoirs are still in a “restriction situation”.



Figure 1. The Paraná River near Corrientes in Argentina on 27 November 2021. Credit: European Union, Copernicus Sentinel-2 imagery.

⁽¹⁾ <https://latinarepublic.com/2022/01/13/the-prolonged-drought-of-the-parana-river/>

This report is an update of Naumann et al. (2021) and focuses on the latest drought conditions in the region, their evolution, their drivers, and their impacts. The relevance of regional efforts for monitoring, forecasting and mitigating the effects of droughts are also discussed.

2 Evolution and status of the 2019-present drought in the La Plata Basin

Naumann et al. (2021) showed that severe, extreme, and exceptional drought conditions were already prevalent in mid-June 2019 in the upper basins of the Paraguay and Paraná rivers in south-central Brazil. According to Naumann et al. (2021) by the end of 2019, drought conditions were fairly extended throughout the Brazilian states of Mato Grosso, Goiás, São Paulo and Paraná, and in Paraguay and central Argentina. During the austral autumn of 2020, the drought persisted (Barbosa et al., 2021) and was subsequently aggravated by an intense heatwave that affected most of central South America between September and October 2020 (Marengo et al., 2021). Dry conditions reached a maximum spatial extent near the end of 2020, when northern Argentina and the Pampas of central-eastern Argentina showed widespread drought conditions. Although the overall dry area subsequently decreased, extreme and exceptional drought was still affecting the upper La Plata Basin at the end of September 2021.

In this section, various indicators are used to characterize the drought event, e.g., the Standardized Precipitation Index (SPI) derived from reanalyses. The areas under different drought categories, derived from combined satellite and in situ data, are used to quantify the spatial extent. Soil moisture indicators are used to characterize availability of water that could have impacts on plants. Other indicators, such as the Fraction of Absorbed Photosynthetically Active Radiation (FAPAR) Anomaly indicator, are used to monitor the impacts on vegetation growth and productivity. Hydrological indicators, such as flow or water level percentiles and deficits, are used to quantify the volume of water deficit in rivers and reservoirs or to monitor whether a required ecological flow or a minimum flow regime is maintained.

2.1 Standardized Precipitation Index (SPI)

The Standardized Precipitation Index is computed with an aggregation period of 9 months (SPI-9) encompassing the warm austral season (September-May). SPI-9 maps show severe dry conditions for three consecutive years (Figure 2). The anomalies detected by SPI-9 values in May 2019 are spotty and not extreme. In contrast, stronger dry conditions developed in the La Plata Basin during the last part of 2019 and persisted for the following three wet seasons (ending in May 2020, May 2021 and May 2022, respectively). The extent of dry conditions encompasses most of the La Plata Basin, including southern Brazil, Paraguay, eastern Bolivia, and northern and central Argentina (Figure 2).

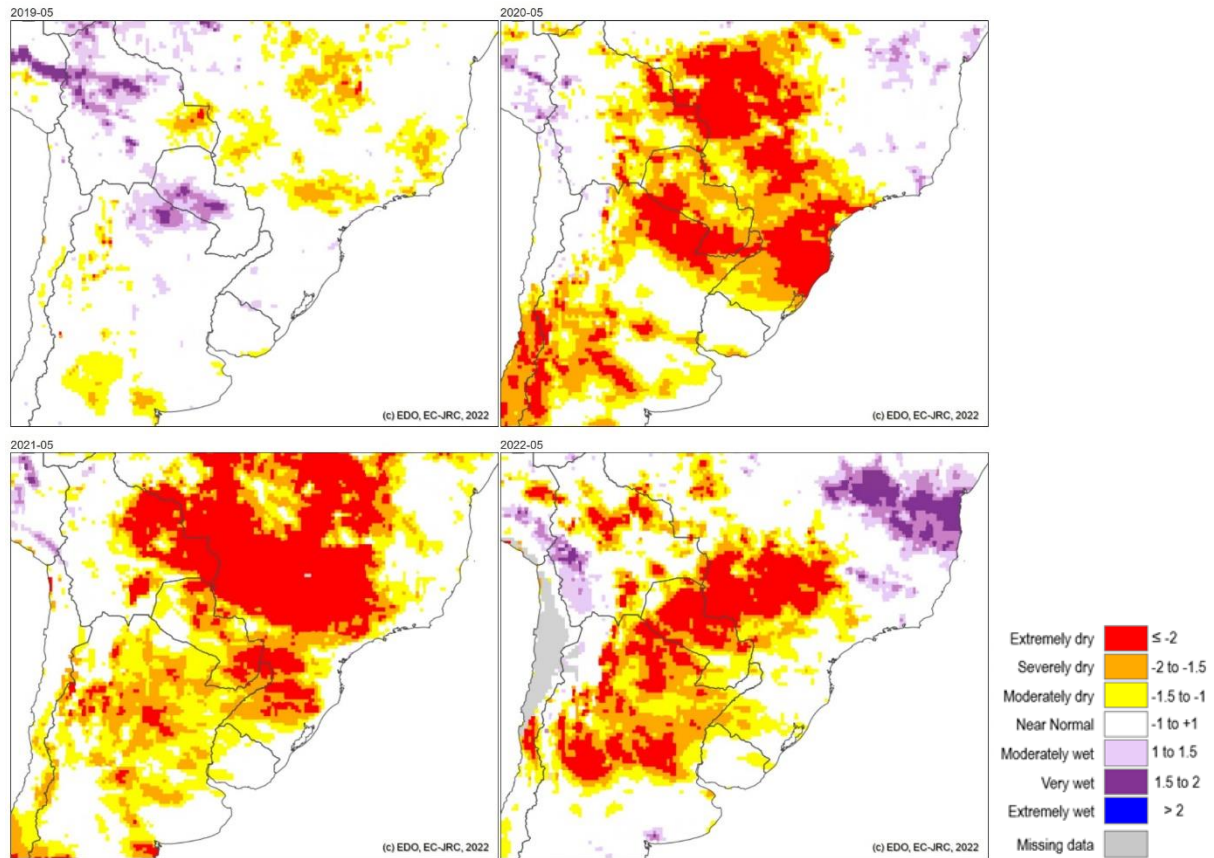


Figure 2. SPI-9 from 2019 to 2022 (accumulation period from September year-1 to May of the year under analysis) based on ECMWF reanalysis ERA5. White areas indicate near-normal conditions, i.e., the index is neither very positive (indicating wet conditions) nor very negative (suggesting dry conditions). Reference baseline: 1991-2020.

2.2 Spatial evolution of areas under different drought categories based on CHIRPS precipitation estimates

In this report, the evolution of the dry event discussed in Naumann et al. (2021) is updated with data from September 2021 to August 2022 (Figure 3). We use maps of drought categories calculated from CHIRPS (Climate Hazards InfraRed Precipitation with Station data) precipitation estimates (Funk et al., 2015) to monitor the temporal evolution of recent drought conditions in the La Plata Basin. CHIRPS maps are derived from both satellite data and *in situ* observations and are produced every pentad (periods of approximately 5 days). CHIRPS data are available since 1981 on approximately a 5 x 5 km grid. The CHIRPS dataset has been validated worldwide, including Brazilian regions where it was found to outperform other precipitation datasets (Marengo et al., 2021).

CHIRPS precipitation estimates are aggregated over 6-month periods ending on the dates shown at the top-right corner of each map in Figure 3. For instance, the “2021-09-15” map (upper left) includes precipitation values for the 6-month period between 16 March 2021 and 15 September 2021. The next panel to the right also corresponds to a 6-month period, but starting and ending one month later (i.e., April to October 2021). A non-parametric approach (Kooperberg and Stone, 1991) was applied to estimate the percentiles of precipitation for each grid cell and date. These percentiles are then used to assign each grid cell and date combination to one of the six drought categories following the U.S. Drought Monitor system (Svoboda et al., 2002). The drought categories range from “non-dry conditions” (percentile values > 30) to “exceptional drought” (percentiles ≤ 2). Figure 3 shows that the extent of areas under extreme and exceptional drought decreased between October and December 2021. Between January and August 2022, however, conditions again worsened: a band of severely to exceptionally dry conditions was present across the northern and western boundaries of the La Plata Basin, from the coastline of São Paulo state in Brazil to northern Argentina and the Paraguayan and Bolivian Chaco, and south along central Argentina. The map for August 2022 shows severe and extreme conditions in the Pampas of central-eastern Argentina, the core crop-producing region.

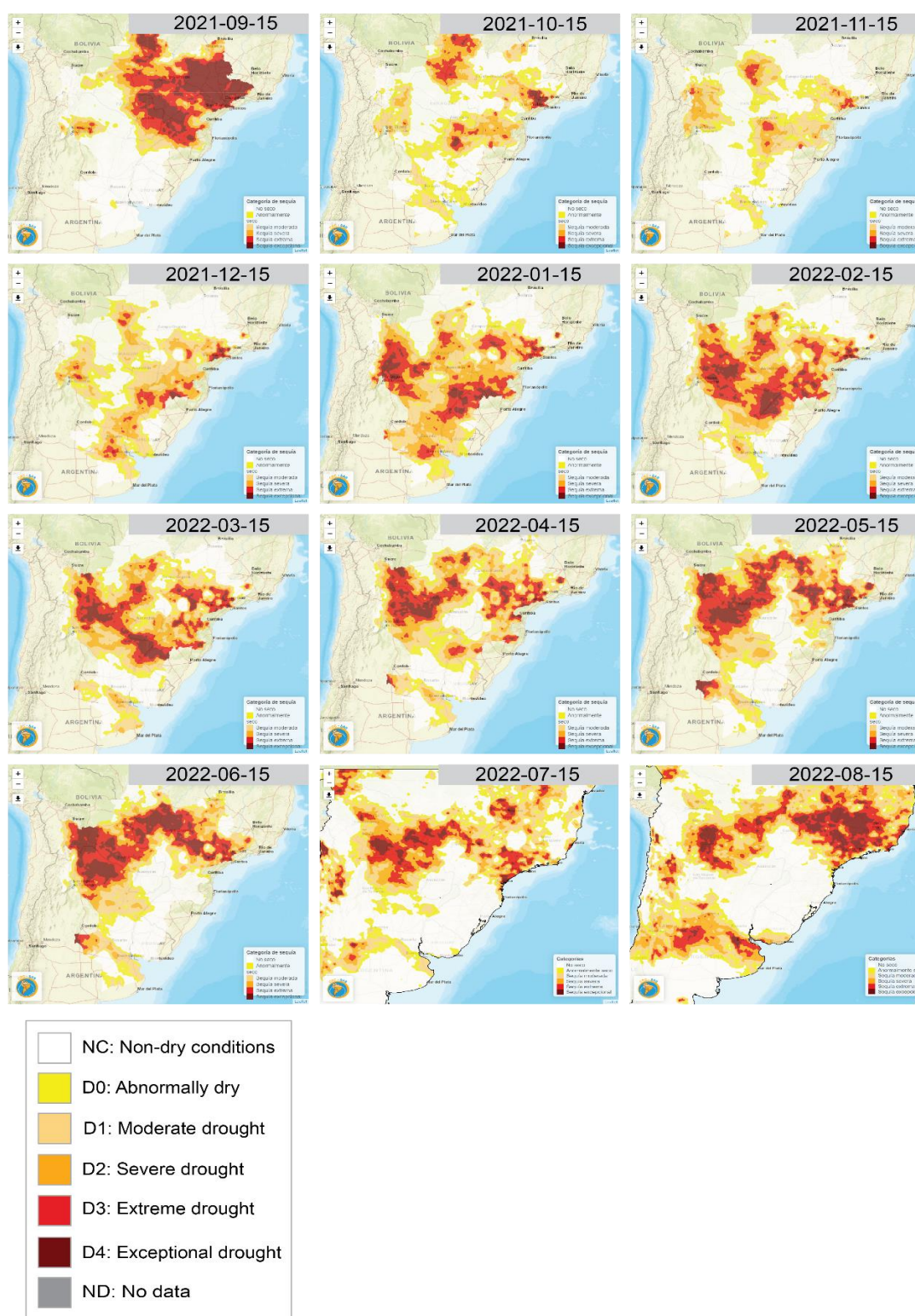


Figure 3. Drought categories for the La Plata Basin derived from CHIRPS precipitation anomalies aggregated by 6-month periods and displayed at monthly intervals covering the period from 15 September 2021 to 15 August 2022. The dates shown in each panel correspond to the end of each 6-month period used to calculate CHIRPS precipitation totals. Source: SISSA.

Figure 4 shows the time series of the proportion of the La Plata Basin area under each drought category, since March 2019. Areas under each drought category were estimated by using CHIRPS precipitation totals for 6-month periods (see discussion for Figure 3). Figure 4 shows that the La Plata Basin had more than half of its area under some drought category (from abnormally dry to exceptional drought) for about three years

(October 2019 to August 2022). The largest spatial extent of dry conditions was reached during the last quarter of 2020, when about three quarters of the La Plata Basin were under drought (Figure 4). There was a sharp decrease in the area under severe and exceptional drought from October 2021 to January 2022 but, subsequently, the severe and exceptional conditions expanded again and lasted through the end of available data in August 2022.

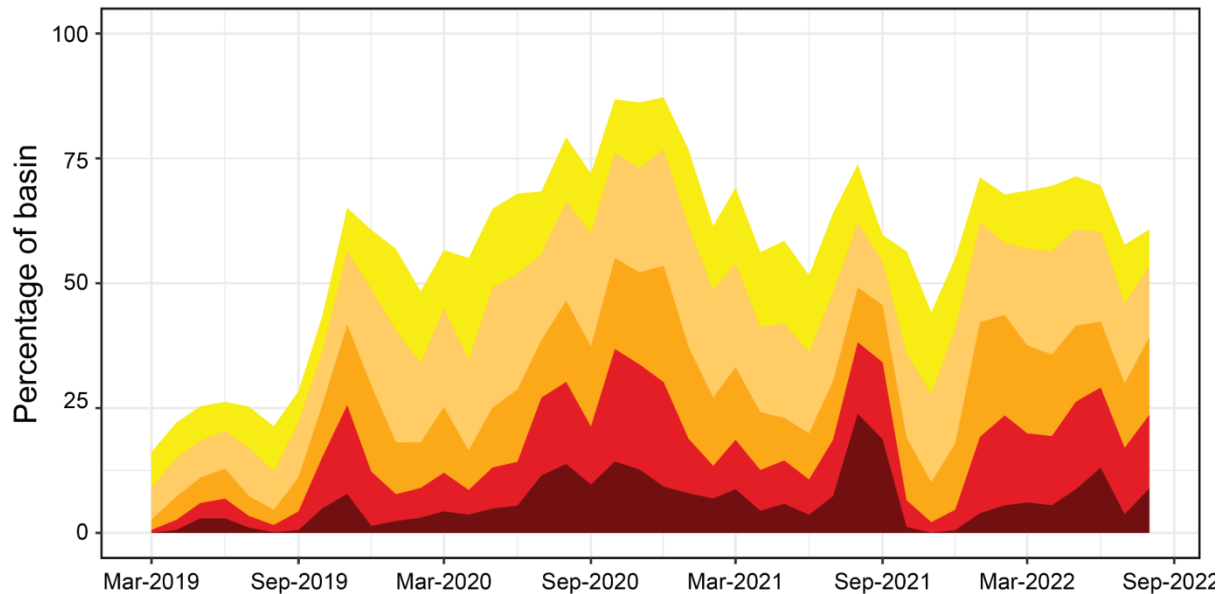


Figure 4. Percentage of area in the La Plata Basin under each of the five drought categories used in Figure 3, from March 2019 to August 2022. The areas were derived from CHIRPS precipitation values aggregated over 6-month periods. For scale and colours, please refer to Figure 3. Source: SISSA.

2.3 Hydrological variables

Lack of precipitation induces a reduction of soil water content. The Soil Moisture Anomaly index (SMA) provides an assessment of such deviations from normal conditions in the root zone water content. It is a direct measure of drought associated with the difficulty of plants in extracting water from the soil. The indicator used here is produced as an ensemble of three datasets: the JRC's in-house LISFLOOD hydrological model (Knijff, Younis, and Roo, 2010), the MODIS-derived land surface temperature (Wan and Li, 1997) and the European Space Agency's (ESA) combined active/passive microwave skin soil moisture (Liu et al., 2012).

The maps of soil moisture anomalies (Figure 5) show close to average (reference period 2001-2017) conditions almost over the entire La Plata Basin at the end of 2018. After a short-wet phase until March 2019, soil moisture has been again dryer than normal although with different intensity and spatial extent. The driest conditions have been observed in March and September 2020, September and December 2021, mainly over southern and south-eastern Brazil, Paraguay, and northern Argentina. In 2022, dry conditions reduced in severity and extent with more variable conditions in time and space. Most critical conditions shifted towards south-west of the regions involved.

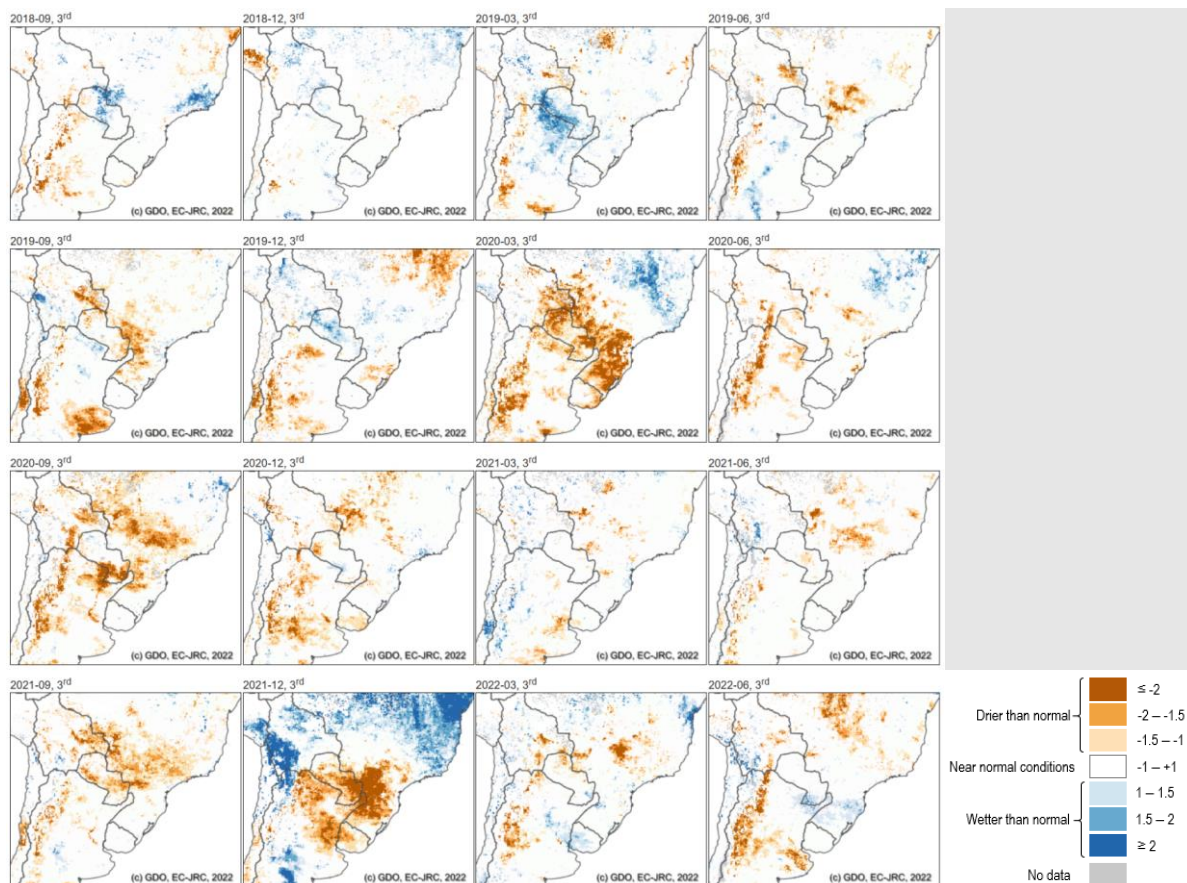


Figure 5. Soil Moisture anomalies (with reference to 2001-2017) across parts of Southern America for the period from September 2018 to June 2022. The maps are represented at the 3rd 10-day period of each month and computed over a 30-day period, hence almost corresponding to a regular month.

The Total Water Storage (TWS) anomaly indicator, implemented in the Copernicus Global Drought Observatory (GDO), is used to detect long-term hydrological drought conditions, emerging when the TWS reaches values lower than normal (reference period 2002-2017). This quantity is often used as a proxy of drought impacts on groundwater. It is computed as anomalies of GRACE-derived TWS data (Cammalleri, Barbosa, and Vogt, 2019), produced by the Center for Space Research (CSR) at the University of Texas at Austin, as scaled by the NASA Jet Propulsion Laboratory (JPL).

As shown in Figure 6, since March 2019 central eastern Brazil has been continuously affected by severe hydrological drought conditions. The maximum extent of the drought area was reached in September 2021 covering most of southern Brazil and a large part of the La Plata Basin.

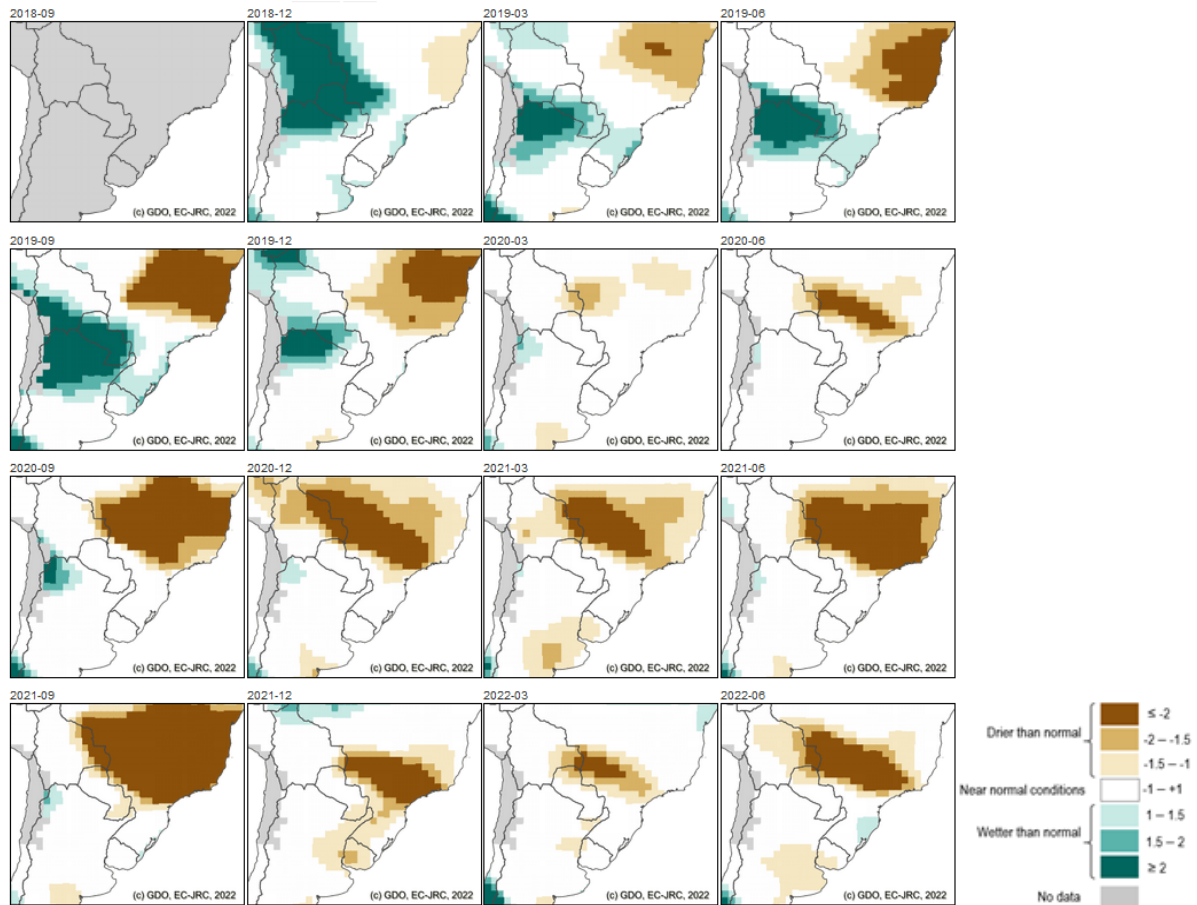


Figure 6. GRACE Total Water Storage Anomaly covering the period from September 2018 to June 2022 (no data is available for September 2018).

2.4 Vegetation response

The Fraction of Absorbed Photosynthetically Active Radiation (FAPAR) Anomaly indicator is used to detect and monitor the impacts on vegetation growth and productivity of environmental stress factors, especially plant water stress due to drought (European and Global Drought Observatories, 2021).

The percentage of the area under different FAPAR and soil moisture anomaly conditions was calculated for some regions under drought conditions, including the Brazilian states of São Paulo and Mato Grosso do Sul, as well as all of Paraguay (Figure 7-9). These regions have been selected having been longer and more severely affected by the drought event. Overall, results show a coherent behaviour of the dynamics of vegetation conditions (upper panels in Figures 7-9) and soil moisture anomaly index (lower panels in Figures 7-9), with an increase in the percentage of dry soils corresponding to a reduction in the photosynthetic activity. Some exceptions in the direct relationship of photosynthetic response to soil dryness can be seen. For instance, in the São Paulo state (Figure 7) from December 2021 to July 2022 some moderate dry events do not correspond to a clear worsening of vegetation conditions. Similarly, in the Paraguay (Figure 9), reduced FAPAR values persist in May-July even after the end of the dry period observed in soil moisture.

These results highlight how a clear response of vegetation greenness to dry conditions can be observed in many cases during the major dry periods, but a general simple relationship between soil moisture and FAPAR anomalies cannot be drawn over the entire region, without accounting for other factors such as the timing of the drought, the local dynamic of vegetation, crop species, phenological stage, soil properties and topography (Vicente-Serrano et al., 2013). More detailed analysis needs to be performed beyond the scope of the present report, to better understand the physical reasons associated with more complex relationships than simple straight coherency.

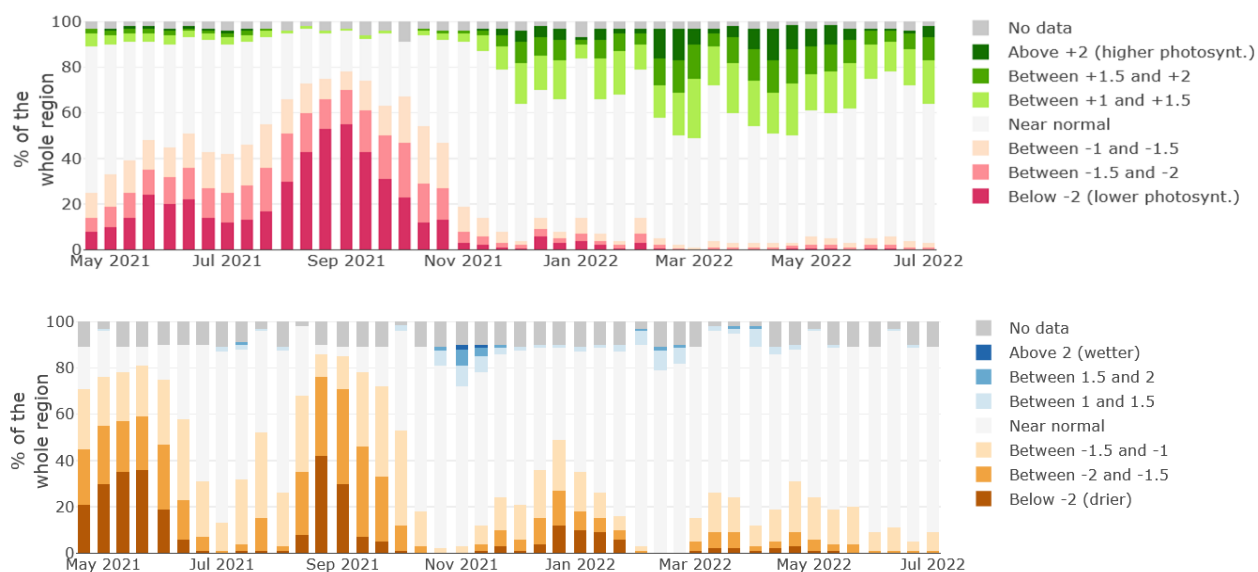


Figure 7. Spatial extent in percentage for FAPAR (upper panel) and Soil Moisture (lower panel) anomalies in São Paulo region. Time series cover the period from May 2021 to July 2022.

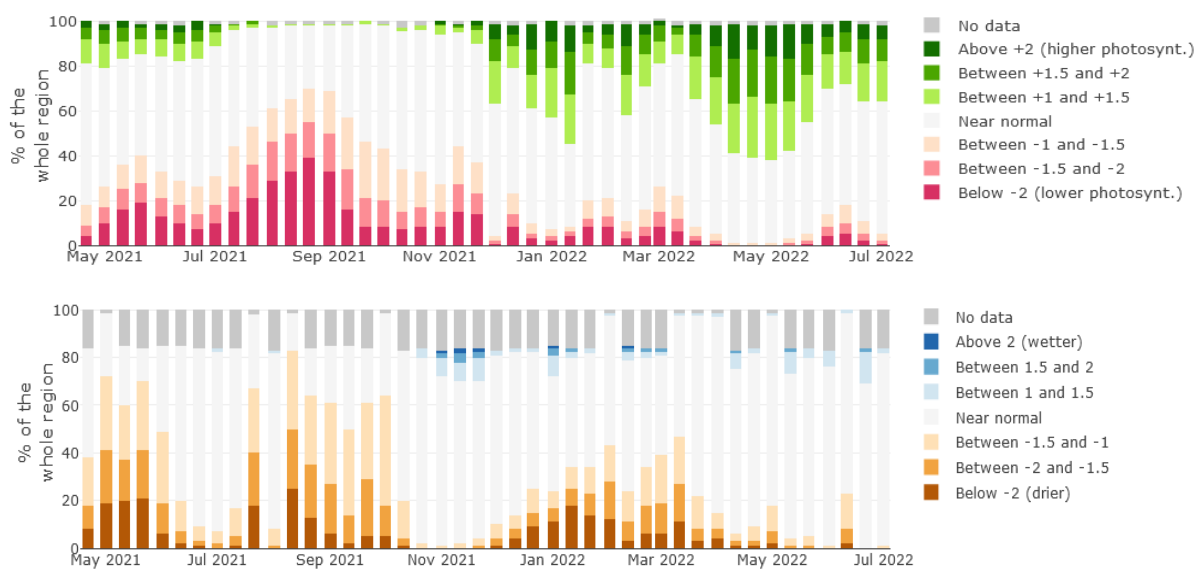


Figure 8. As Figure 7, but for the Mato Grosso do Sul region.

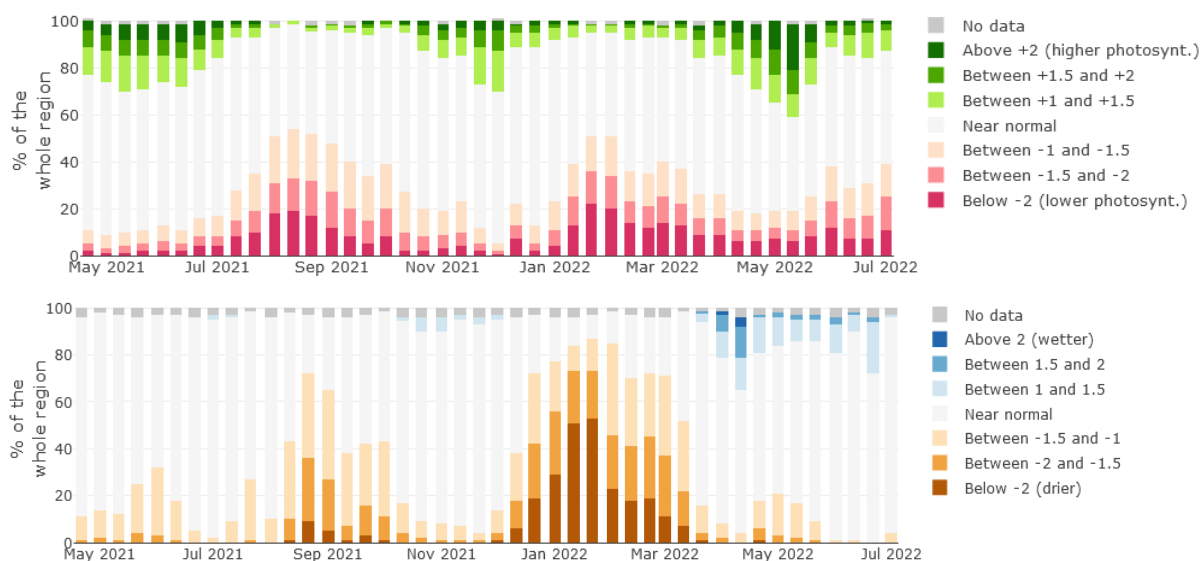


Figure 9. As Figure 7, but for Paraguay.

2.5 Streamflow indicators of drought conditions

This section relies on standardized streamflow indicators to characterize drought conditions in the upper and middle portions of the La Plata Basin.

2.5.1 Paraná River streamflow at Corrientes, Argentina

Precipitation deficits across the northern part of the La Plata Basin have been prevailing for several years. In particular, the low precipitation amounts observed in recent years during the usually wet summer season, have triggered a steady decrease in the amount of water stored in both surface and underground reservoirs. As a result, there has been a considerable decrease in the base streamflow of the Paraná River entering the Argentine territory (Figure 1). Figure 10 shows a time series of the Standardized Streamflow Index (SSFI) for the Paraná River at Corrientes, Argentina. As Corrientes is downstream of the confluence of the Paraná and Paraguay rivers, the streamflow captures conditions in the upper La Plata Basin. The SSFI was calculated fitting gamma distributions to the 1971-2021 streamflow series for each month of the year and then expressing gamma percentiles as z scores (Vicente-Serrano et al., 2012).

Low standardized streamflow values ($SSFI < 0$) were initially observed in mid-2018 and have been steadily present since mid-2019, reaching peak extreme values in mid-2021 ($SSFI < -2$). In 2022, SSFI values began to rise in February and reached stable values around -1 during April-June 2022. The rise in SSFI values was tied to spatially patchy positive rainfall anomalies (still surrounded by negative anomalies) during early 2022. The positive rainfall anomalies became more widespread in March 2022 but subsequently reverted to localized negative anomalies during the austral fall. These positive anomalies – which contributed to the partial recovery of Paraná streamflow in 2022 – were concentrated on the unregulated portion of the Paraná basin and the Iguazú basin.

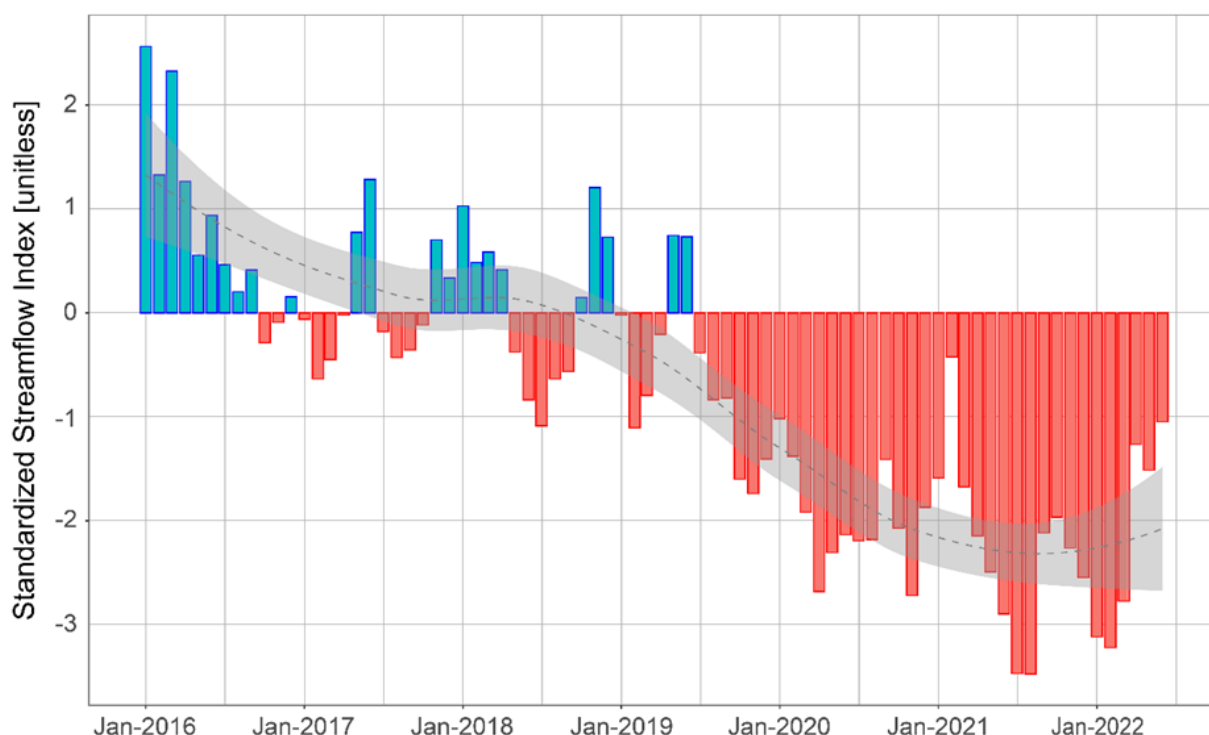


Figure 10. Standardized Streamflow Index (SSFI) at Corrientes, Argentina, from January 2016 to June 2022. Negative SSFI values (red bars) indicate negative streamflow anomalies. The dashed grey line shows the smoothed trend and the associated confidence interval. Source: Instituto Nacional del Agua, Argentina.

2.5.2 Streamflow at Emborcação, Furnas, Jurumirim, Foz do Areia and Itaipu hydro-power plants in the Upper Paraná River

Figure 11 shows the time series of the SSFI values for four locations in the upper La Plata Basin where important hydro-power plants (HPPs) are located. SSFI values have been calculated for two different aggregation scales: 12 (left column, Figure 11) and 24 months (right column, Figure 11). Figure 11 suggests that the discharges of the Paraná River reflect the recent dry conditions in the La Plata Basin, with SSFI values falling far below average.

The Emborcação (Paranaíba river basin) and Furnas (Grande River basin) HPPs located in the north-eastern Paraná River Basin have been facing a hydrological drought, classified as severe ($SSFI < -1.3$) and exceptional ($SSFI < -2.0$) since 2014. However, during the latest austral summer (October 2021 – March 2022), intense rainfall events in the south of the state of Bahia and the north of Minas Gerais state led to an improvement in the hydrological drought conditions. Since February 2019, stream-flows at the Jurumirim (Paranapanema river basin) and Foz do Areia (Iguazu River basin) HPPs have been in a hydrological drought condition, between severe and exceptional. At the time of writing, the HPP Jurumirim remains in the most critical situation ($SSFI-12 = -2.2$ and $SSFI-24 = -3.4$). The inflow at Itaipu HPP has been facing a hydrological drought since April 2019 and has been in an exceptional drought condition since December 2020 ($SSFI < -2.0$). This hydrological drought condition configures as the most severe since January 1981 ($SSFI-12 = -2.3$ and $SSFI-24 = -3.2$).

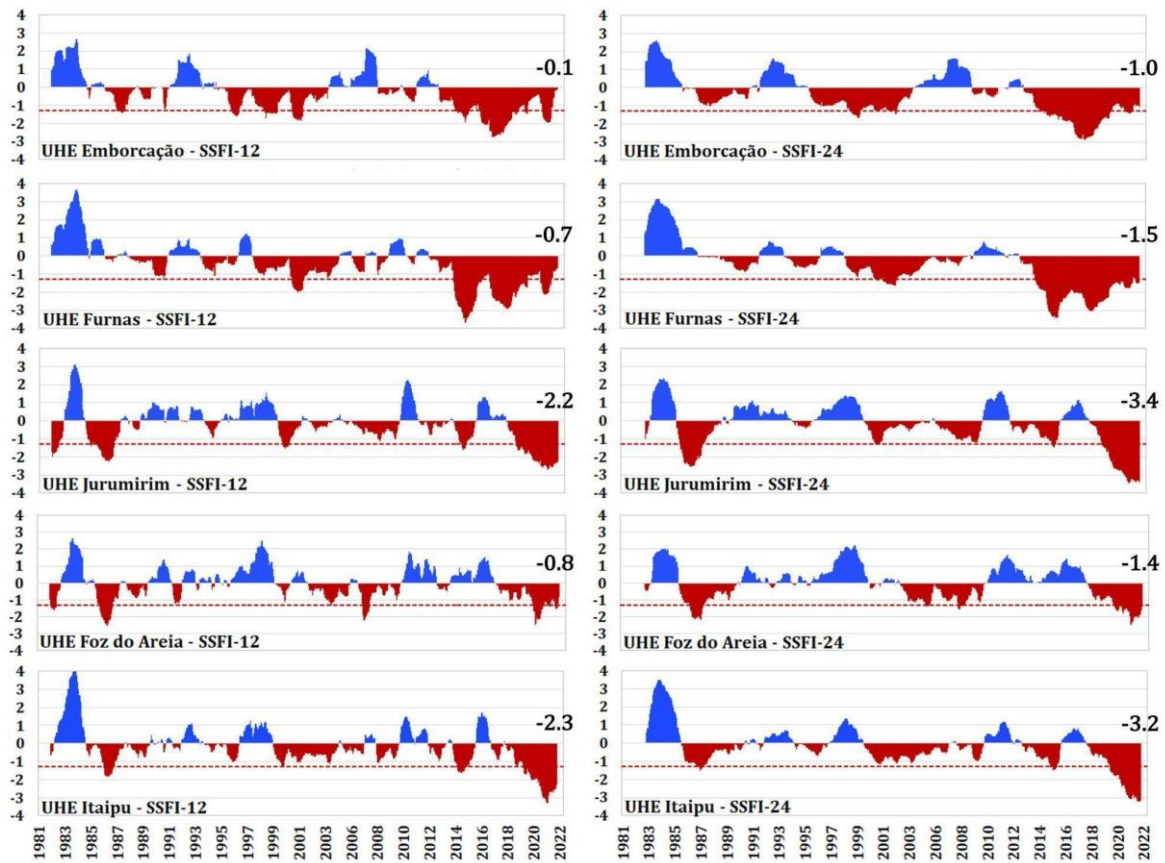


Figure 11. Standardized Streamflow Index (SSFI) covering the period 1981 until June 2022, at time scales of 12 months (left panel) and 24 months (right panel), for the HPP in the sub-basins of Emborcação, Furnas, Jurumirim, Foz do Areia and Itaipu. Source: CEMADEN.

2.6 Monitoring drought using combined indicators: the JRC Combined Drought Index

The Combined Drought Index (CDI; Cammalleri et al., 2021) is an agricultural drought indicator developed by the JRC, which is based on the causal relationship between lagged precipitation deficits, soil moisture anomalies (SMA) and the fraction of Absorbed Photosynthetically Active Radiation anomalies of plants. The CDI has 6 categories: Watch, Warning, Alert, Temporary Soil Moisture Recovery, Temporary FAPAR Recovery and Full Recovery. The CDI has a global coverage with a spatial resolution of 1°x1°, and it is updated 3 times per month.

An evaluation of the CDI over the Pampas of central-eastern Argentina is ongoing, focused on a regional assessment of the association between CDI drought categories and soybean and maize yields and agricultural emergency declarations (Spennemann et al., 2022).

Figure 12 shows the evolution of the CDI in four months (Oct-Nov-Jan-Feb) within the warm season (September-March) of 2021-2022. During October 2021 (upper row, Figure 12), the CDI shows Alert category in parts of the South Atlantic Convergence Zone (SACZ), with a lower spatial extent in south-western Brazil, north-western Paraguay and central Chile. In addition, precipitation deficits over several areas of the LPB were triggering the Watch category. During November 2021 (second row), the CDI showed over the SACZ region a reversion to the Watch category; while an increase of the area under Alert category in the south-west of Brazil and east of Bolivia was observed. During this period, the area under the Warning category started to increase in central Argentina. During January 2022 (third row), precipitation deficits showed an intensification in south-eastern Brazil, Uruguay, and central-eastern and north-eastern Argentina. These deficits were accompanied by strong negative soil moisture anomalies resulting in a Warning category over those regions. During February 2022 (last row), the north-eastern region of Argentina remained under the Warning category, and a spatial increase of the Watch category over Brazil was observed.

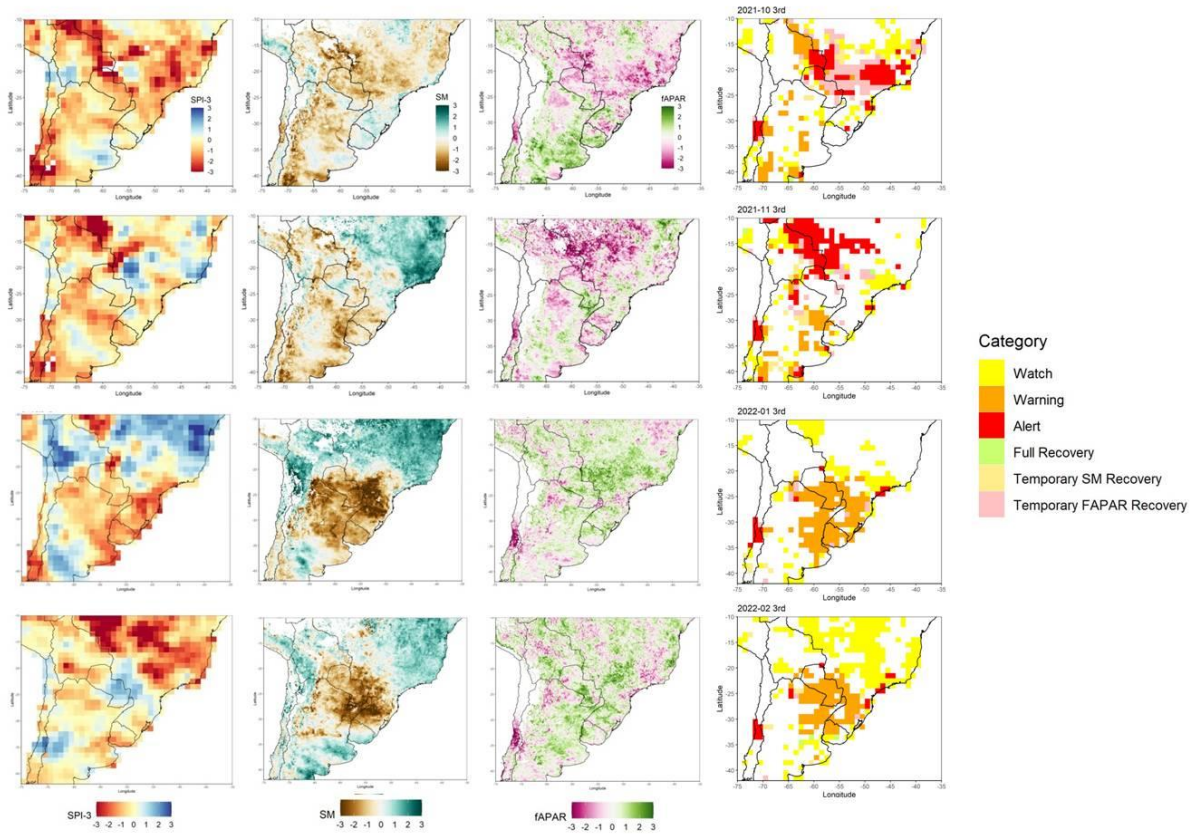


Figure 12. Combined Drought Index (CDI) for Oct-Nov-Jan-Feb of the warm season 2021-2022. The CDI is shown on the rightmost column, while the first three columns on the left show the indicators that contribute to the index calculation: Standardized Precipitation Index (SPI-3, first column from the left), Soil Moisture Anomalies (SMA, second column), and FAPAR Anomalies (third column). Adapted from Spennemann et al., 2022.

2.7 Summary of drought conditions

Before introducing the predicted evolution of this multiannual event simulated by seasonal forecasts, we show a summary of conditions at the time of writing (end of September 2022, Figure 13)

The SPI-3 map (left panel in Figure 13) shows wide regions in the central and southern part of the La Plata Basin where precipitation from July to September 2022 are far below the average, suggesting dry meteorological conditions.

Soil moisture (central panel in Figure 13) appears to be wetter than normal in the upper part of the La Plata Basin in the Brazilian Mato Grosso do Sul and Mato Grosso states, as well as in the Pantanal. Nonetheless, extensively dryer-than-normal conditions are reported in the lower basin (southern part), confirming that the region has not recovered yet from drought.

FAPAR (right panel in Figure 13), shows close to normal or higher than normal values in a wide region including north-eastern Argentina, southern Brazil, and Uruguay. Elsewhere normal to lower-than-normal values are observed.

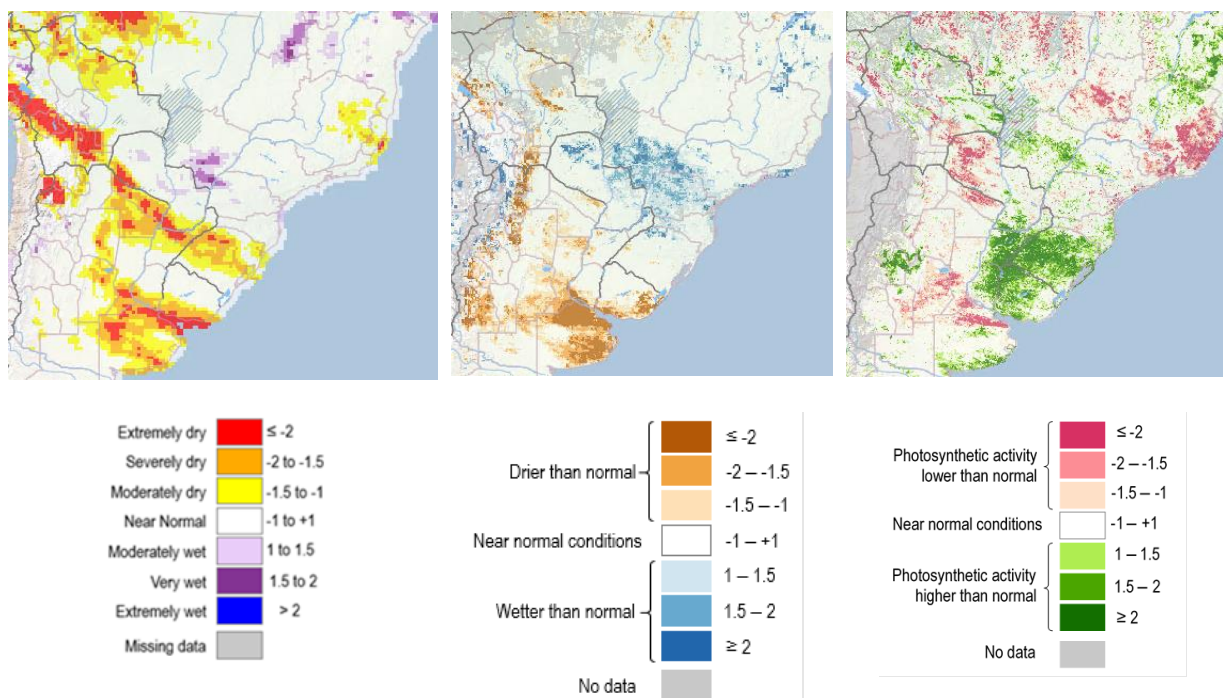


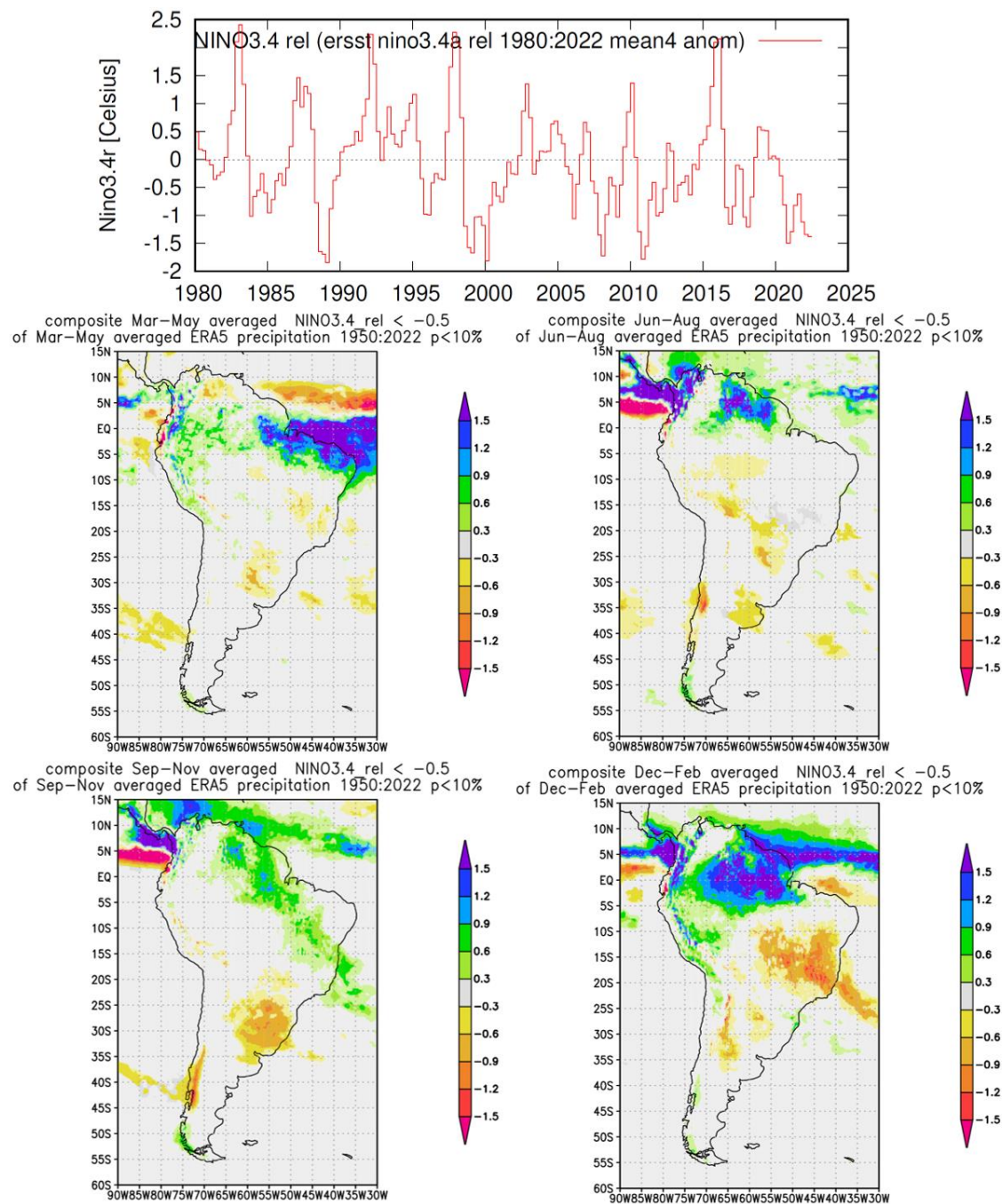
Figure 13. SPI-3 (left), SMA (central), FAPAR Anomalies (right) at the end of September 2022.

3 Associated circulation patterns and seasonal and decadal outlooks

3.1 Seasonal prediction and outlook

Gomes, Cavalcanti, and Müller, (2021) reported the presence of a persistent pattern of west-east convection anomalies in the tropical Pacific related to stable conditions observed in the region from September 2019 to March 2020. Moreover, they reported that the extreme positive phase of the Indian Ocean dipole during the austral spring of 2019 could have influenced temperature and precipitation in South America via a wave propagation from the Indian Ocean to the South American continent.

Dominant large-scale climatic drivers of seasonal precipitation in southern South America such as El Niño Southern Oscillation (ENSO) and the Antarctic Oscillation (AAO; Silvestri and Vera, 2009) have been in a phase that favours drought in the LPB since 2020 (Figure 14 and Figure 15). Using the composite analysis for both ENSO and AAO indices, a clear reduction of the LPB precipitation during austral spring and summer emerges for negative ENSO and positive AAO phase, but also impacting the other seasons. During austral summer the reduction in the LPB precipitation is more marked for the AAO than for ENSO, while during austral winter the ENSO signal is stronger.



² Confidence level is a measure of the reliability of a result, that is, e.g., a confidence level of 0.90 means that there is a probability of at least 90% that such result is reliable. The p-values are computed assuming normal distributions, which means that they should only be considered a rough estimate of the significance.

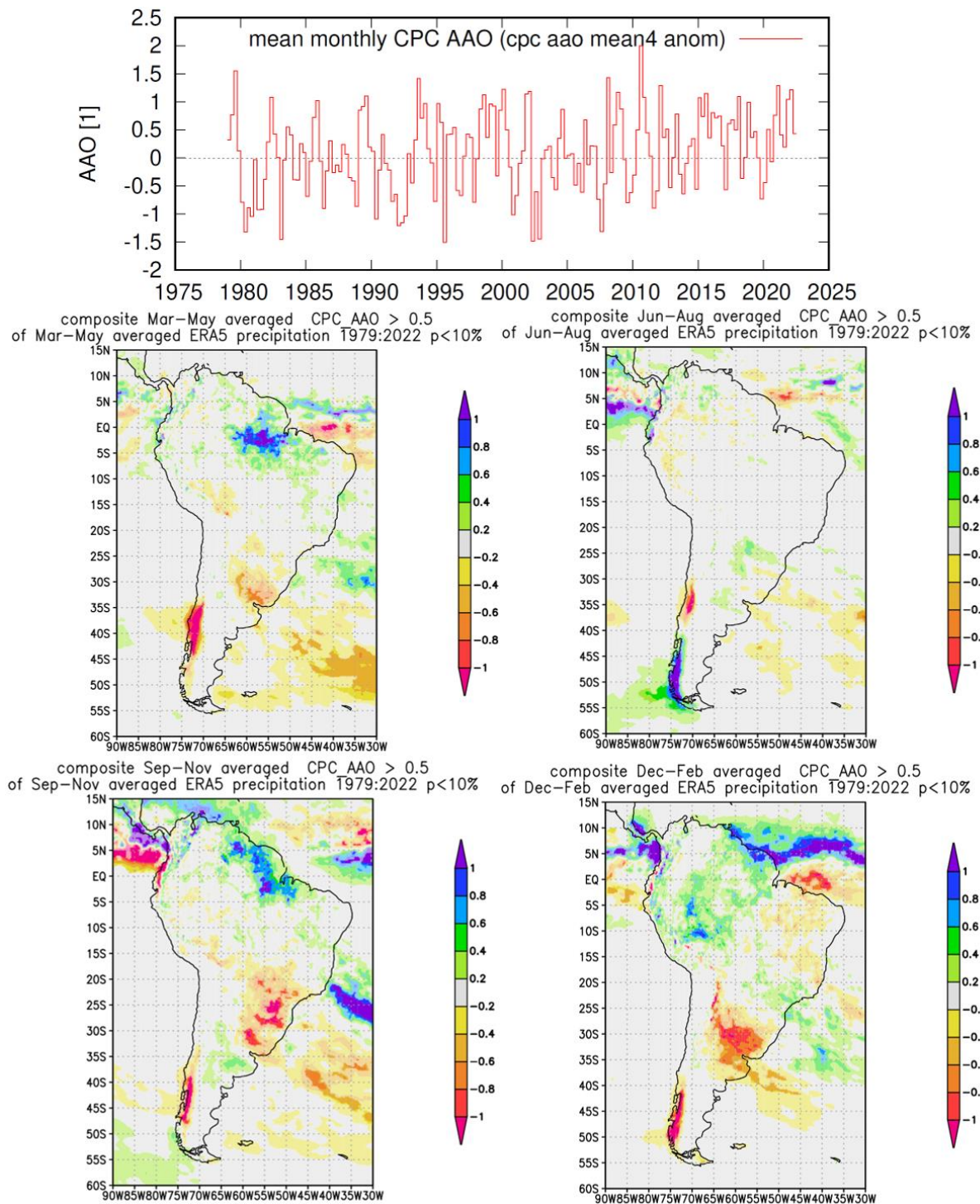
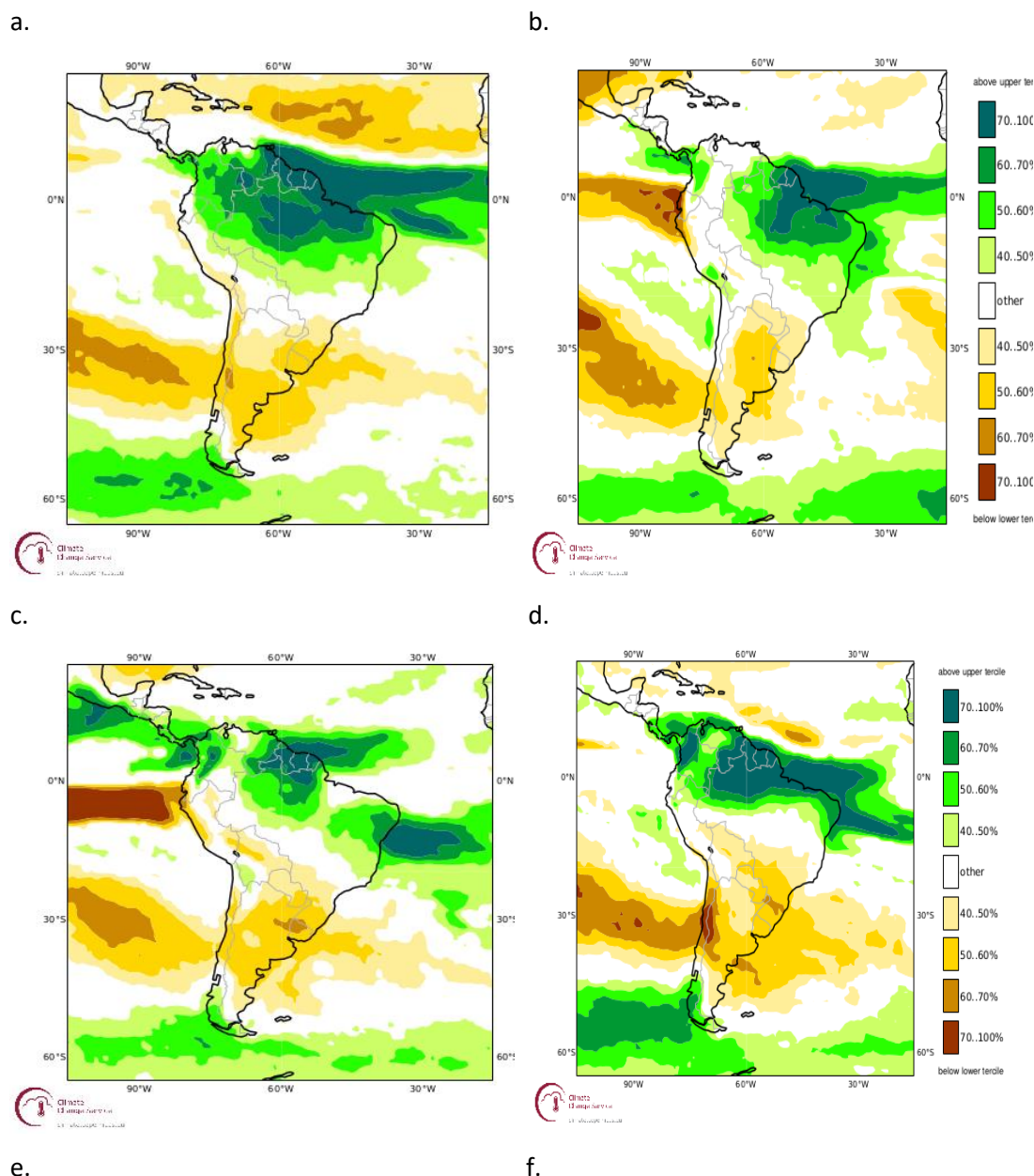


Figure 15. Same as Figure 14, but for the positive Antarctic Oscillation - AAO ERA5 precipitation composites (mm/day) based on CPC-NOAA index above 0.5 in the period 1979-2022. Source: WMO-KNMI climate explorer <https://climexp.knmi.nl>.

Naumann et al., (2021) and Gomes, Cavalcanti, and Müller, (2021) identified the El Niño-Southern Oscillation phenomenon as one of the main driving factors of the dry event in the La Plata Basin. Since the analysis done for the 2021 LPB drought report, seasonal forecast models continuously forecast higher chances for below-normal precipitation anomalies over the LPB (Figure 16) as a response to negative anomalies in the tropical Pacific Ocean associated with persistent La Niña conditions (Figure 17).

At the time of writing conditions in the tropical Pacific continue to show negative ocean surface temperature anomalies, consistent with La Niña phase of ENSO. In fact, according to the “ENSO blog” from NOAA⁽³⁾, June 2022 temperature anomaly over the Niño 3.4 region ranks as the 7th strongest negative value since 1950. In addition, the Southern Oscillation Index (SOI) has been increasing its value in recent months (Figure 17) indicating that the atmospheric coupling to the ocean in the tropics is very strong. Both indications, plus the current ENSO forecast (Figure 18), suggest that the chances of persisting La Niña conditions during the austral spring and summer of 2022-23 are above 50%. Consequently, a third consecutive spring and summer with La Niña conditions may be experienced; the last time such an event happened was in 1998-2001.

Seasonal forecasts also predict higher chances for the occurrence of the negative phase of the Indian Ocean Dipole (IOD) from October 2022 to March 2023 (Figure 18). The IOD is positively correlated with the state of ENSO and has its peak in spring. In its negative phase, the IOD is associated with negative precipitation anomalies over the LPB (Gomes, Cavalcanti, and Müller, 2021). The modulation of ENSO teleconnections by the negative IOD could affect the expected precipitation anomalies in the LPB. Consequently, seasonal forecasts for the upcoming months point to higher chances for precipitation below normal over the LPB region.



⁽³⁾ <https://www.climate.gov/news-features/blogs/july-2022-la-niña-update-comic-timing>

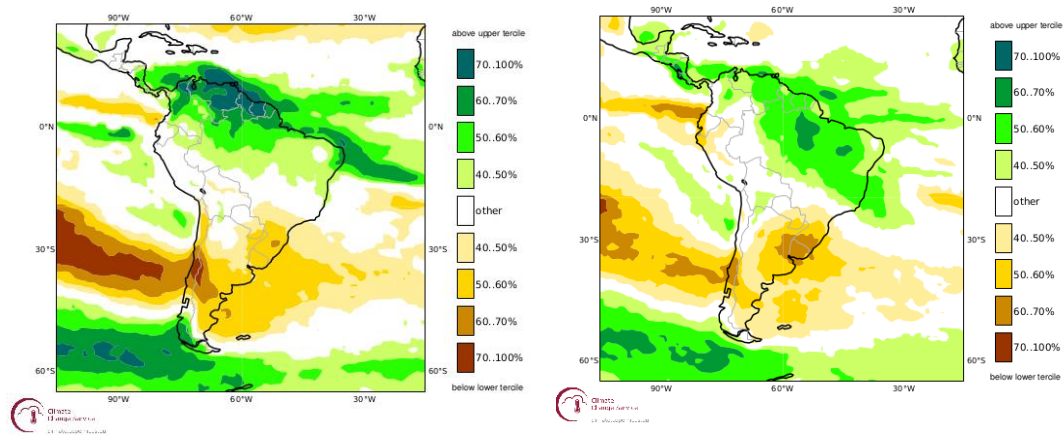


Figure 16. Probabilistic precipitation forecasts for (a) SON 2021, (b) DJF 2021/2022, (c) MAM 2022, (d) JJA 2022, and (e) ASO 2022, f) OND 2022 from initial conditions of August 2021, November 2021, February 2022, May 2022, July 2022 and September 2022 respectively. Forecasts were elaborated with the Copernicus Climate Change Service (C3S) multi-model system. Precipitation categories are defined by the terciles of the distribution (below normal, near normal and above normal). The figure shows only the most likely category for each grid point. Thus, brown colours denote highest chances for below normal precipitation, while green values correspond to higher chances for above normal precipitation. White colours indicate higher chances for precipitation near normal or equal probabilities for the terciles. Source: Copernicus Climate Change Service⁽⁴⁾.

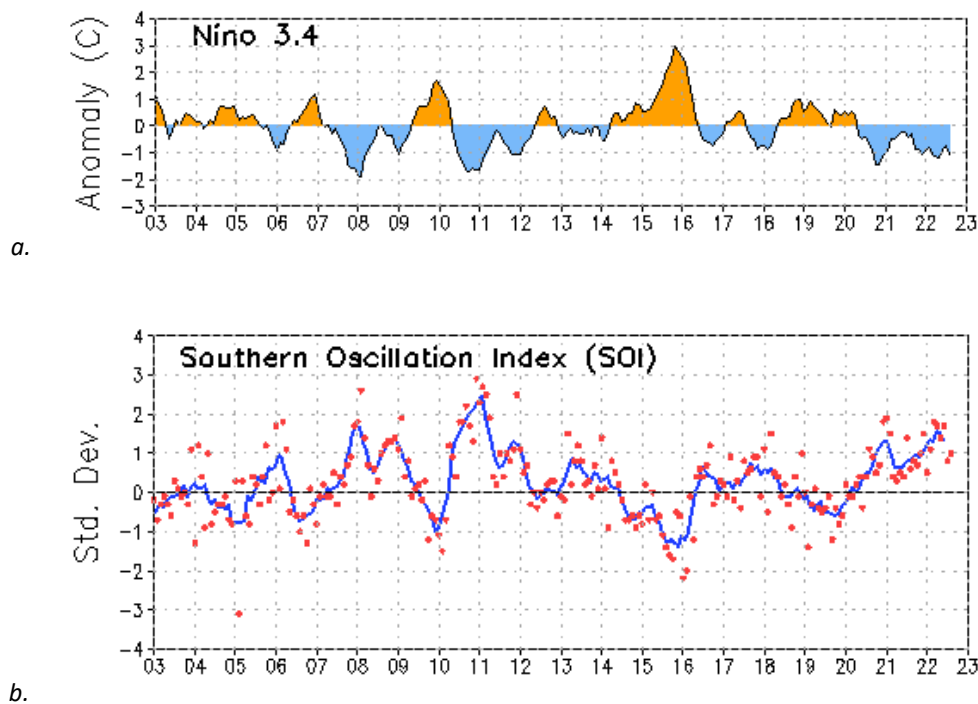


Figure 17. (a) Niño 3.4 index, calculated as the area-averaged sea surface temperature anomalies (°C) at 5N-5S, 170W-120W. Source: NOAA, CPC⁽⁵⁾, (b) Monthly evolution of the Southern Oscillation Index defined as the standardized sea-level pressure anomaly (hPa) differences between Tahiti and Darwin (SOI, dots) and five-month running mean (lines). Source NOAA, CPC⁽⁶⁾. Data from 2003 updated through August 2022.

⁽⁴⁾ https://climate.copernicus.eu/charts/c3s_seasonal/

⁽⁵⁾ <https://www.cpc.ncep.noaa.gov/products/CDB/Tropics/figt5.shtml>

⁽⁶⁾ <https://www.cpc.ncep.noaa.gov/products/CDB/Tropics/figt1.shtml>

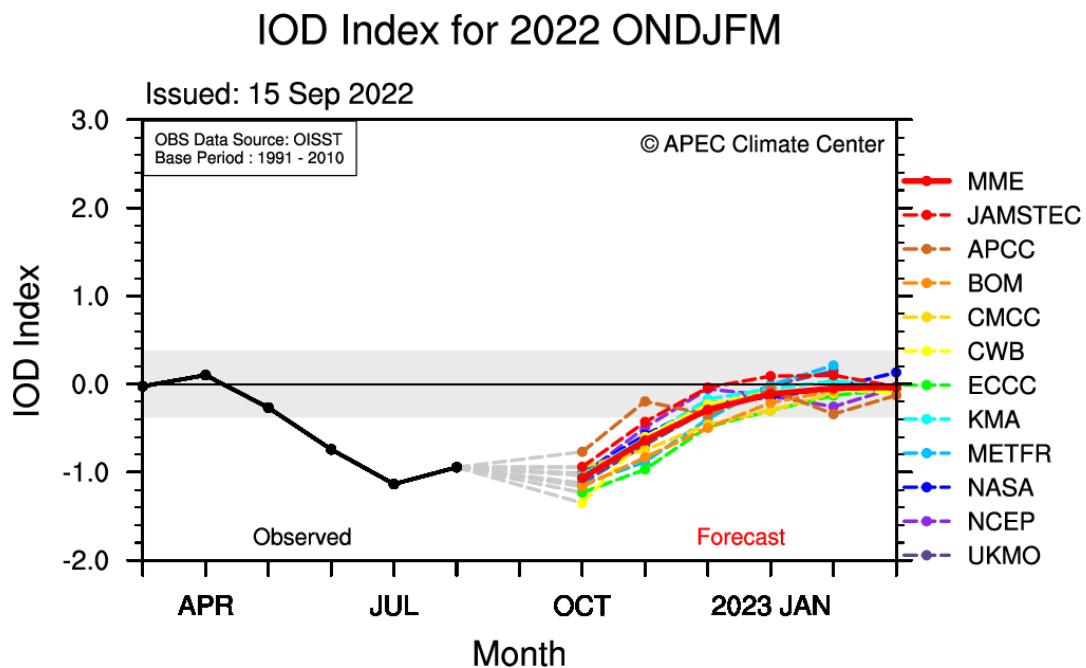
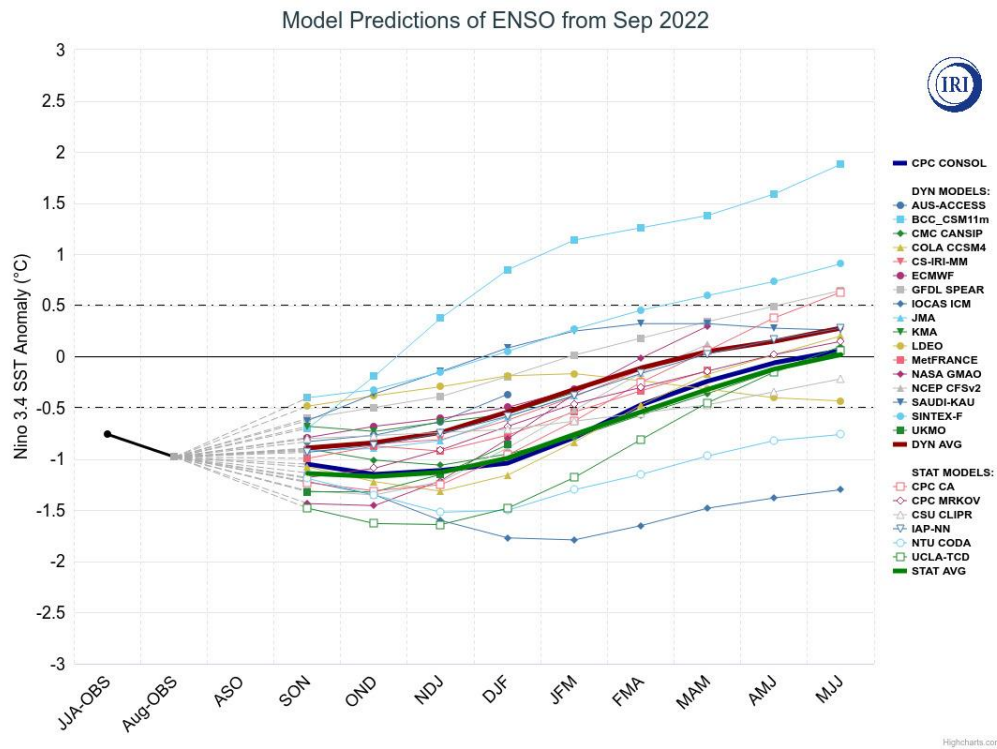


Figure 18. Upper panel: Time series of predicted sea surface temperature anomalies for the Niño 3.4 region (in degrees C) from various dynamical and statistical models for nine overlapping 3-month periods from ASO 2022 to MJJ 2023. Lower panel: Time series of predicted sea surface temperature anomalies for the Indian Ocean Dipole region (in degrees C) from various dynamical models for seven months. Source: International Research Institute for Climate and Society (IRI)⁽⁷⁾ and APEC Climate Center⁽⁸⁾

⁽⁷⁾ https://iri.columbia.edu/our-expertise/climate/forecasts/enso/current/?enso_tab=enso-sst_table.

⁽⁸⁾ <https://www.apcc21.org/ser/enso.do?lang=en>

3.2 Decadal prediction

Decadal climate predictions are issued on a yearly basis and are produced by initializing a suite of numerical prediction models from a state which is consistent with the observed climate state and integrating them forward in time typically up to ten years (Meehl et al., 2021). Decadal predictions aim to capture the evolution of climate due to external forcing (e.g., greenhouse gases, aerosols, etc.) and slowly evolving natural climate variability (e.g., Pacific and Atlantic Decadal Variabilities, etc.). Despite common limitations such as low signal-to-noise ratios and limited predictability in many regions, decadal predictions display high skill in predicting climate in the North Atlantic, Indian Ocean and western Pacific regions. Decadal predictions offer a view of the climate in the coming years/decade that can serve as a key source of information for strategic decision making to a wide range of public and private stakeholders in areas such as agriculture, water management, civil protection, energy and infrastructure management and planning, among others.

On decadal timescales, two important climate variability modes, the Atlantic Multidecadal Oscillation (AMO) and the Pacific Decadal Oscillation (PDO) are in a phase that favours lower-than-average precipitation in the LPB as depicted by the composite analysis shown in Figure 19. WMO decadal predictions from contributing centres show a 2022-2026 multi-model mean lower than average precipitation over most of South America including the Paraná-upper LPB. The predicted anomalies resemble the composites from a positive AMO phase. The AMO is predicted to continue in a positive phase for the period 2022-2024 (Figure 20). Additionally, the PDO is predicted to continue in a negative phase for the period 2022-2024, possibly also favouring negative precipitation anomalies in LPB (Figure 20) in the coming years (Hermanson et al., 2022).

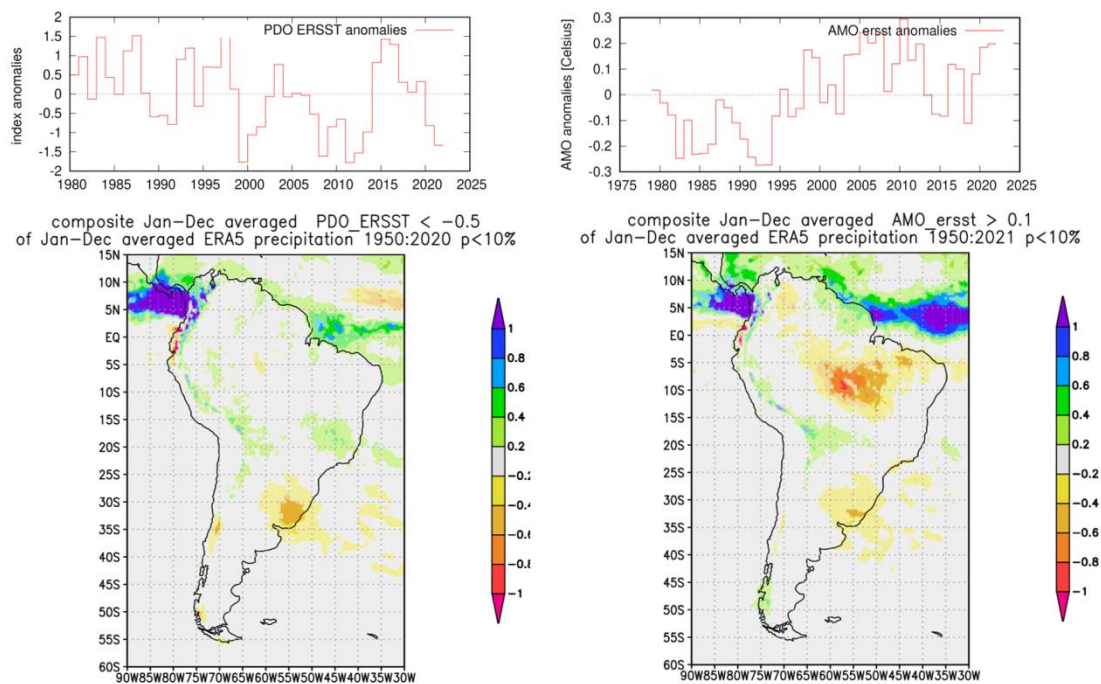


Figure 19. Upper Panel: Annual mean Pacific Decadal Oscillation - PDO (left) and Atlantic Multidecadal Oscillation – AMO (right) indices (Extended Reconstructed Sea Surface Temperature, ERSST). Lower Panel: Annual ERA5 precipitation composites (mm/day) in South America for PDO values below -0.5 (left) and AMO values over 0.1 (right). Period of analysis 1950-2021. Source: WMO-KNMI climate explorer <https://climexp.knmi.nl>.

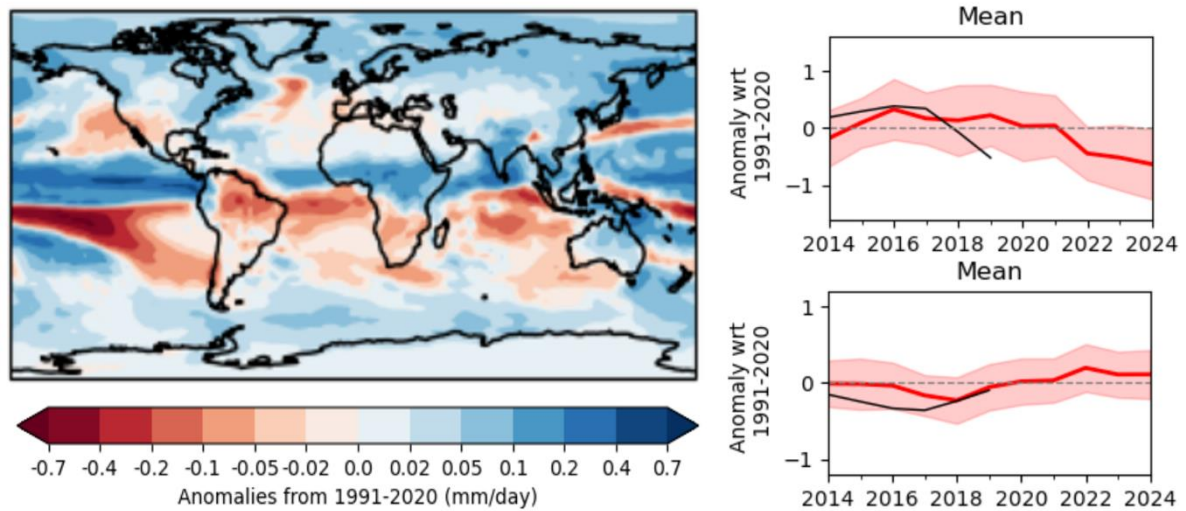


Figure 20. Left: WMO multi-system mean precipitation predictions for 2022-2026 in models initialized in 2021. Top right: WMO multi-system mean (red line), spread (shading) predicted PDO index in models initialized in 2021. Bottom right: WMO multi-system mean (red line), spread (shading) predicted AMO index in models initialized in 2021. Black lines represent the observed values. Source: <https://hadleyserver.metoffice.gov.uk/wmolc/>.

4 Reported impacts of the present drought

The persisting drought situation in the La Plata Basin in 2021 and 2022 had impacts on ecosystems and several important socioeconomic sectors of the affected countries (Argentina, Brazil and Uruguay) including agriculture, inland water navigation, energy production, and water supply. The previous JRC report on the La Plata Basin (Naumann et al., 2021) described impacts during the first part of this dry event. This section updates the consequences of the continuing dry event.

4.1 Ecosystems – Wetlands

The persistent drought has affected ecosystems and communities along the middle and lower course of the Paraná River. Fish populations in the region are highly vulnerable to drought because many of the wetlands (which serve as breeding grounds for the animals) are unavailable, causing fish numbers to dwindle (Noticias Ambientales, 2021). Furthermore, stagnant waters can lower oxygen content in the water which also affects aquatic species. The decline in fish population has also become a serious obstacle for the fishermen who rely on the fauna of the Paraná for their livelihoods ⁽⁹⁾.

During the summer seasons 2020-21 and 2021-22, microorganisms that release toxins potentially harmful to human health turned the waters of the Paraná, Uruguay and La Plata rivers into greenish-bluish colour. This phenomenon is the result of cyanobacteria blooms and originates from the excessive concentration of nutrients (from sewage drains, industrial residues and fertilizers) tied to the extraordinary decrease of the Paraná River streamflow and the arrival of the warm months in southern South America (Noticias Ambientales, 2022). Though the Argentine Federal Council of Sanitary Services Entities (COFES) – the entity that groups organizations that provide drinking water – declared to have adequate technology to guarantee the safety of drinking water, fishing and water sports and activities were all prohibited during summer 2020-2021 (Parana hacia el Mundo, 2022).

In February 2022, the Argentine Ministry of Health issued an alert for the presence of cyanobacteria that could cause nasal congestion and gastroenterocolitis (Cuevas, 2022). These bacteria can also lead to dehydration in children who play on the shore, and, rarely, severe hepatotoxic adverse reactions such as liver or neurological conditions, of which first manifestation may be an intense headache. The Environmental Observatory of the Argentine National University of Rosario (Observatorio Ambiental de la Universidad Nacional de Rosario) issued an alert about fluorescent spots in the Paraná River caused by cyanobacteria. Also because of low Paraná levels, City of Rosario authorities encouraged the population to use drinking water responsibly, to ensure an adequate supply for daily consumption (Ambito, 2022).

4.2 Fires

One important ecological consequence of the extended drought event in the La Plata Basin was the widespread occurrence of forest, crop, and rangeland fires in the province of Corrientes in north-eastern Argentina during mid-January to March 2022. Corrientes is part of the Mesopotamia (“between rivers”) region of Argentina, as it is bound by the Paraná (on the west) and the Uruguay (on the east) rivers. Corrientes is a highly productive agricultural province. The main agricultural activities are cattle farming (4.6 million heads), citrus, tobacco, tea, and yerba mate. Forestry is a very important activity, with pine and eucalyptus plantations covering large areas in the north of the region.

The northern and central parts of the province of Corrientes include unique biodiverse region: the Iberá Wetlands (Esteros del Iberá, in Spanish), one of Argentine largest wetlands (Mata, Buitenwerf, and Svenning, 2021). The Iberá wetlands encompass a mosaic of marshes, swamps, grasslands, savannas, and gallery forests with an area of approximately 14,000 km². The Iberá wetlands also include the last remaining large areas of subtropical grasslands in South America. Due to their ecological importance, the Iberá Wetlands have been included in the Ramsar Convention on Wetlands to guarantee their future conservation (Grimson et al., 2013). The area is protected by national park and conservation areas of the Province of Corrientes. The protected wetlands include mammals such as anteaters, the Aguaráguazú (*Chrysocyon brachyurus*), the Pampas deer

⁽⁹⁾ <https://es.mongabay.com/2021/08/parana-el-plata-cuenca-rios-sequia-argentina-brasil-paraguay/>

(*Ozotoceros bezoarticus*), capybaras or “carpinchos” (*Hydrochoerus hydrochaeris*), reptiles like the yacare caiman (*Caiman yacare*) and broad-snouted caiman (*Caiman latirostris*), and several bird species.

Rainfall deficits starting in 2020, together with high temperatures and low rainfall in January-February 2022 contributed to the large number of fires throughout Corrientes. The wetlands gain most water from precipitation, and the flat topography induces a predominantly vertical balance between precipitation, evapotranspiration and infiltration within the system. During normal times, about 40% of Corrientes is covered by water; however, because of low rainfall (about 10% of the normal amount fell in January 2022) only 15% of the province was under water in early 2022 (Hiba, 2022). The low rainfall was accompanied by extremely warm temperatures in early 2022: the city of Corrientes (capital of the province) experienced a heat wave lasting 13 days (from January 14th to the 26th) with daily maximum temperatures reaching 42.6 °C (Agrositio, 2022).

To illustrate the rapidly evolving drought conditions that favoured fires, Figure 21 shows a time series of the Standardized Precipitation Evaporation Index for a temporal scale of 3 months (SPEI-3; Vicente-Serrano, Beguería, and López-Moreno, 2010) in Mercedes, near the centre of the province of Corrientes. Although during January 2022 the SPEI-3 already showed drought conditions (values < -0.5), there was a rapid intensification of dry conditions during February 2022: the SPEI-3 decreased from -0.77 on 31 January to -3.00 (SPEI values are truncated at this number) on 5 March 2022.

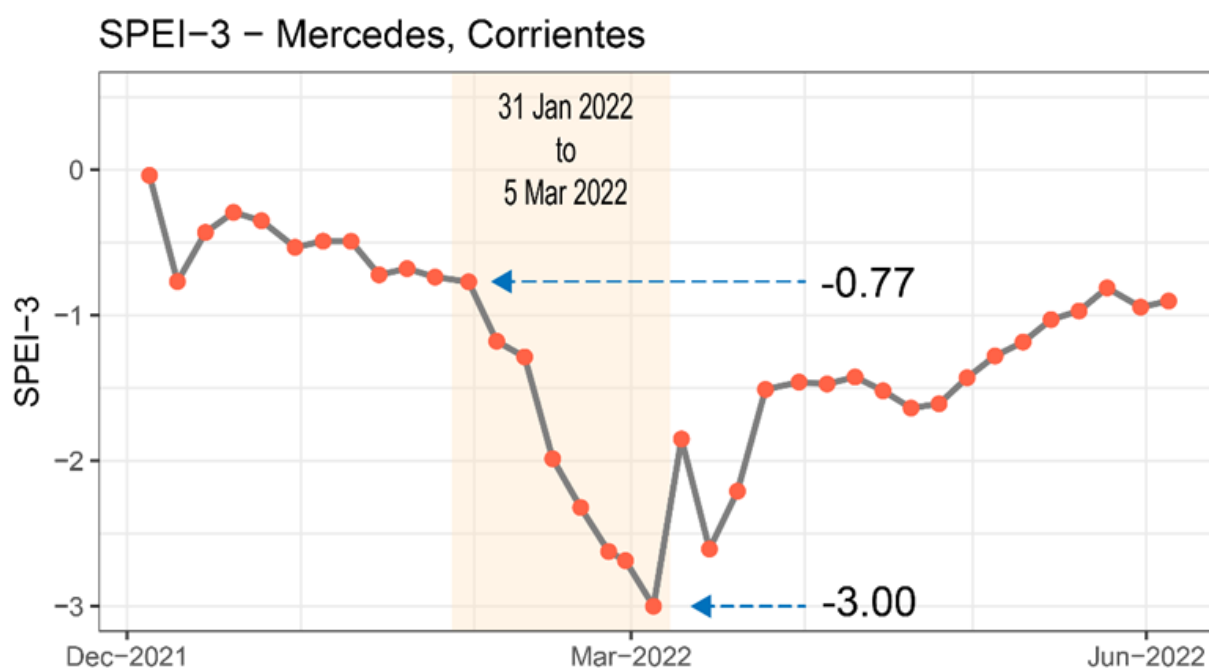


Figure 21. Time series of SPEI-3 values at a meteorological station operated by Argentine agricultural research institute (INTA) near Mercedes, Corrientes. The sharp decrease during February 2022 (shaded area) is well visible. Note that SPEI-3 values lower than -3.00 are truncated for display purposes. Source: SISSA.

Figure 22 shows percentiles of the Evaporative Stress Index (Anderson et al., 2016) for the four weeks ending on 29 January 2022 (i.e., just before the sharp decrease in SPEI-3). The ESI can identify regions where vegetation is stressed due to lack of water, capturing early signals of drought without using observed rainfall data. The ESI is based on satellite observations of land surface temperature, which are used to estimate water loss due to evapotranspiration (ET). Figure 22 shows that the entire province of Corrientes (approximately indicated by the white bold line) and surrounding areas recorded ESI values in the lowest decile of the historical distribution, as well as areas to the southwest and northeast of the province. These very low ET rates suggest that the atmospheric demand of water could not be satisfied due to inadequate soil moisture and therefore vegetation was highly stressed.

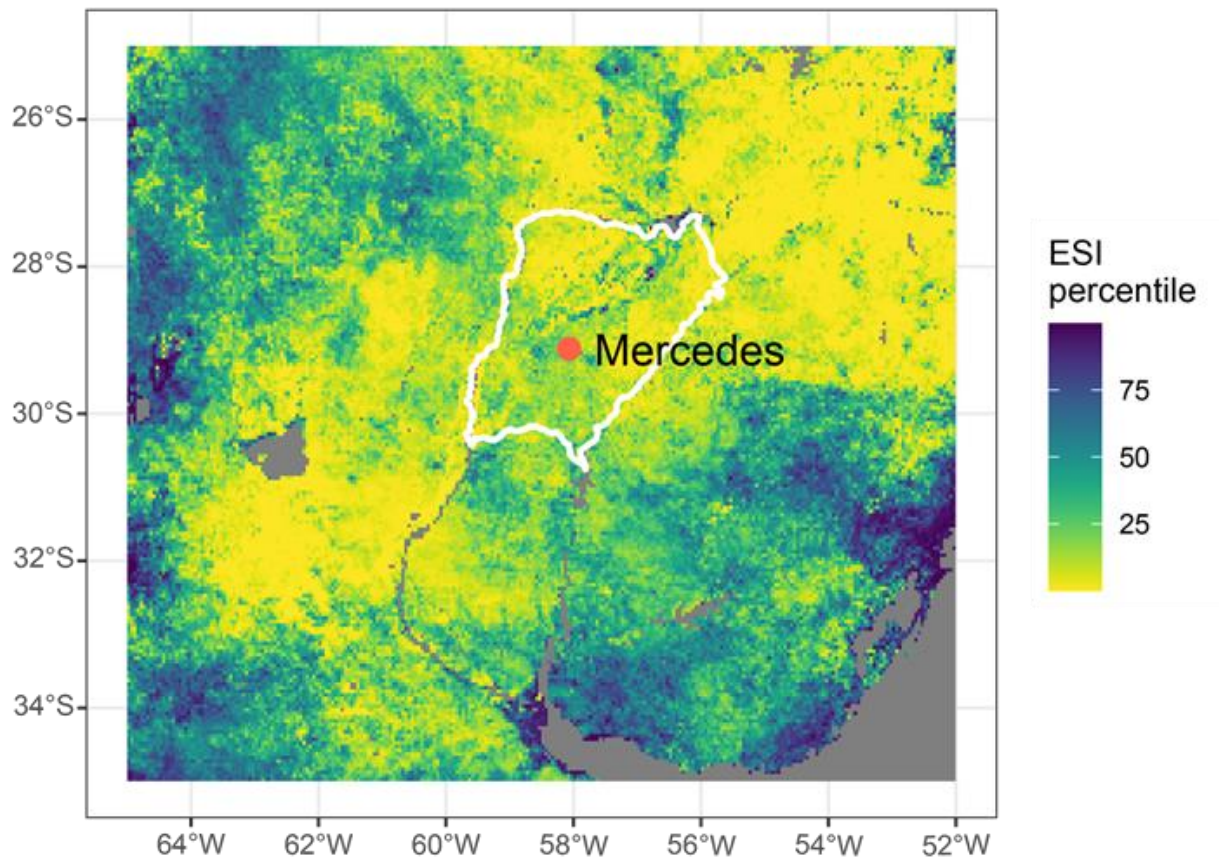


Figure 22. Evaporative Stress Index (ESI) percentiles for the 4-week period ending on 29 January 2022. The white bold line indicates the Province of Corrientes, and the red dot denotes the location of the Mercedes INTA meteorological station for which SPEI-3 values were shown in Figure 21. Source: SISSA.

The fires began in the central part of Corrientes and moved northward. A map (Figure 23) produced by Argentine Agricultural Research Institute (INTA) showed that at the end of February 2022 over one million hectares were burnt (Saucedo, Perucca, and Kurtz, 2022). At its peak, the fires encompassed about 14% of the province of Corrientes and 40% of the Iberá National Park (Arias, 2022). Most of the burned area (about one third) corresponded to wetlands; another 30% of the affected area corresponded to grazing lands in the northern part of Corrientes (Centenera, 2022). Both planted and natural forests represent about 7% of the total area burned.

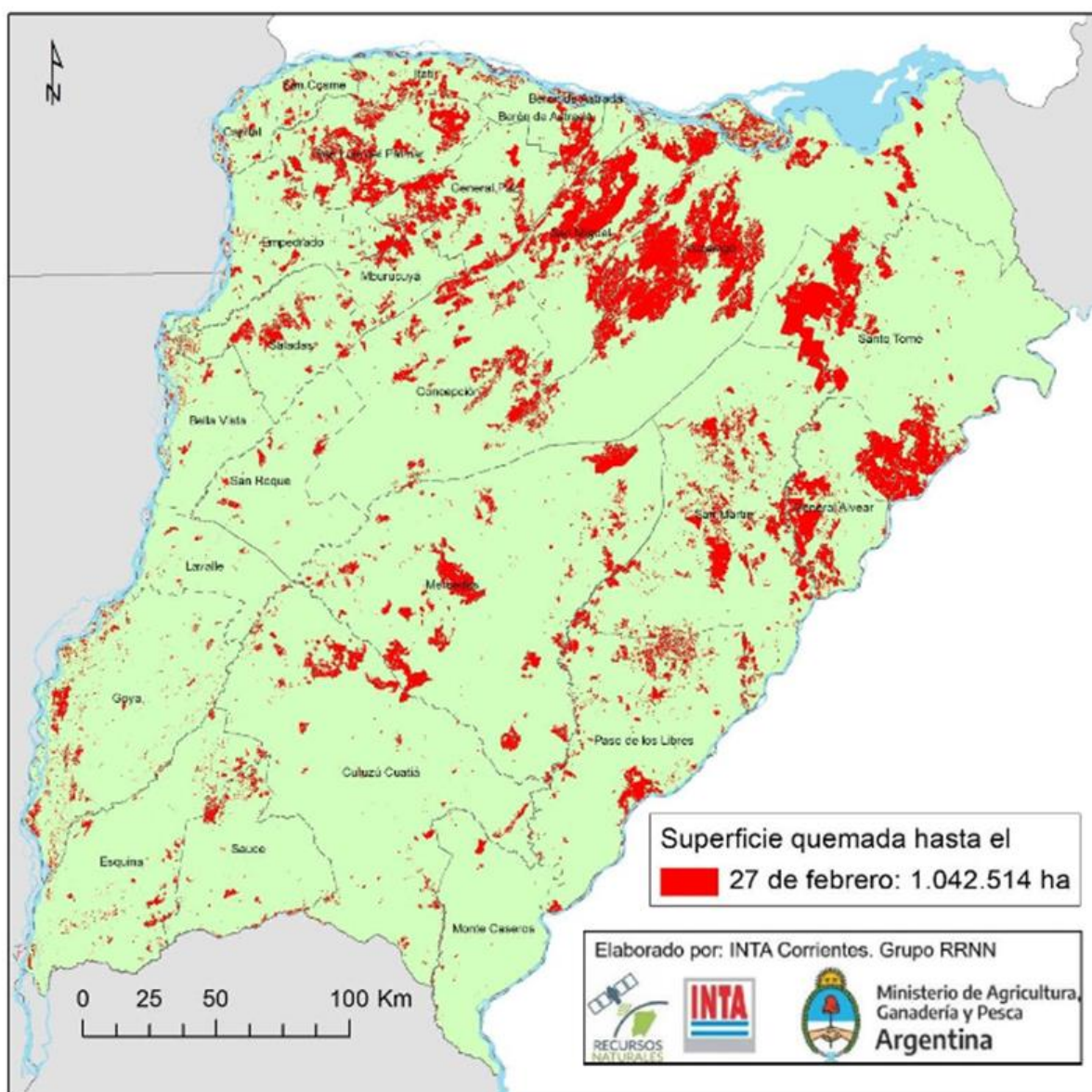


Figure 23. Areas burned in the Province of Corrientes, Argentina by 27 February 2022. Source: INTA Corrientes (see Saucedo et al. 2022).

The ecological impacts of the drought-related Corrientes fires are still being assessed. However, many wild animals were unable to escape the fires and perished. Other long-lasting impacts are expected. For instance, several hundred kilometres of wire fencing were destroyed, resulting in cattle invading protected park areas and competing with wildlife for food and water; rebuilding this infrastructure (possibly replacing wooden posts with non-combustible materials) will take time and require financing. Fortunately, rainfall in early March 2022 contributed to mitigate fires. By mid-March 2022 the Iberá National Park reopened, and there have been reports of an initial re-greening of burnt areas and a return of wild fauna. On the other hand, the productive impacts of the Corrientes fires also remain to be quantified in detail. Early reports in late February 2022 (while fires were still active) estimated losses at about 232 million USD, but the estimate is likely to rise quickly. Estimated impacts have included significant losses of cattle and slower growth and affected reproduction due to lost availability of forage. About half of the yerba mate production in Corrientes (30% of Argentine production) has been lost. Rice production (about 45% of Argentine production) has been compromised due to low availability of water for inundation of the field. The forested area affected was a relatively small portion of the total, but losses in these areas were total.

4.3 Crops, Livestock and Economy

Dry conditions in late 2021 and early 2022 were most apparent in north-eastern Argentina, the portion of the country that is encompassed by the Plata Basin. The austral summer 2021/2022 was among the driest and warmest recorded. In contrast, the core agricultural region of central-eastern Argentina known as the Pampas showed lower impacts from dry conditions at that time – impacts were concentrated in a few dispersed areas. As a result, impacts were relatively minor on nationally aggregated statistics for the main summer crops (soybeans and maize) that are mainly produced in the Pampas. Argentine Directorate for Agricultural Statistics Dirección de Estimaciones Agrícolas⁽¹⁰⁾ reported that despite a 2021/22 sown area (that was 900,000 hectares higher than the previous cycle due to favourable costs and market conditions) national maize production decreased by 2.5%. For soybean, the 2021/22 total production is estimated to be about 4.8% lower than the previous cycle. Fortunately, high market prices for these commodities partially offset the economic impacts.

The economic impacts on agricultural production systems were among the highest in recent years for the north-eastern Argentina provinces for which declarations of agricultural emergency and disaster were issued. Agricultural losses and damages were estimated at about 3.78 million USD by Argentine Directorate for Agricultural Risk and Emergencies (Dirección Nacional de Riesgo y Emergencias Agropecuarias). The largest share of losses and damages were associated with cattle production, followed by field crop production, production of fruits and vegetables, forestry, and dairy production. Some of the damages corresponded to activities very important to regional economies, such as cotton production in Formosa, or tobacco, tea, and yerba mate in Misiones. Although monitoring reports routinely report artisanal fisheries among the sectors showing impacts from dry conditions, the north-eastern provinces did not formally report economic impacts on this activity.

According to provincial declarations of agricultural emergency and disaster, the main impacts of dry conditions affected cattle production systems: over 60 % of total damages and losses were tied to this activity (OMEGA, 2022). At the peak of dry conditions in January 2022, about 6.9 million heads of cattle were affected. Impacts on cattle include the direct effects from lack of drinking water and intense heat on the health and wellbeing of animals, as well as decreased forage availability in natural grasslands and implanted pastures (OMEGA, 2022). Reduced forage availability created additional costs because of the need to purchase supplemental feed and to reduce stocks through forced sales. Local reports suggest widespread occurrence of lowered pregnancy rates and deteriorated body condition, particularly for cows nursing calves. Nevertheless, no widespread cattle mortality was reported. However, delayed impacts are expected throughout 2022 because of poor body conditions of cattle, and reduced availability of feed during the austral winter. As described elsewhere in this report, cattle production infrastructure such as wire fences and drinking water systems were affected by intense fires, particularly in the province of Corrientes. This resulted in widespread mixing of animals from different farmers, and unmanaged grazing by wondering cattle.

During the austral fall and winter of 2022, dry conditions expanded from north-eastern Argentina to the Pampas of central-eastern Argentina (Figure 24). The Pampas had been somewhat less affected by the austral summer drought. The intensification of dry conditions throughout the Pampas during the austral fall-winter of 2023 has had (and is likely to continue having) severe impacts on wheat. Argentine Bolsa de Cereales (Grain Exchange) reported that the area sown with wheat (grown mainly in the Pampas) decreased by 600,000 hectares or about 9% with respect to the previous cycle; final impacts on wheat production will emerge after harvest in late 2022.

⁽¹⁰⁾ <https://www.magyp.gob.ar/sitio/areas/estimaciones/monitor/index.php>

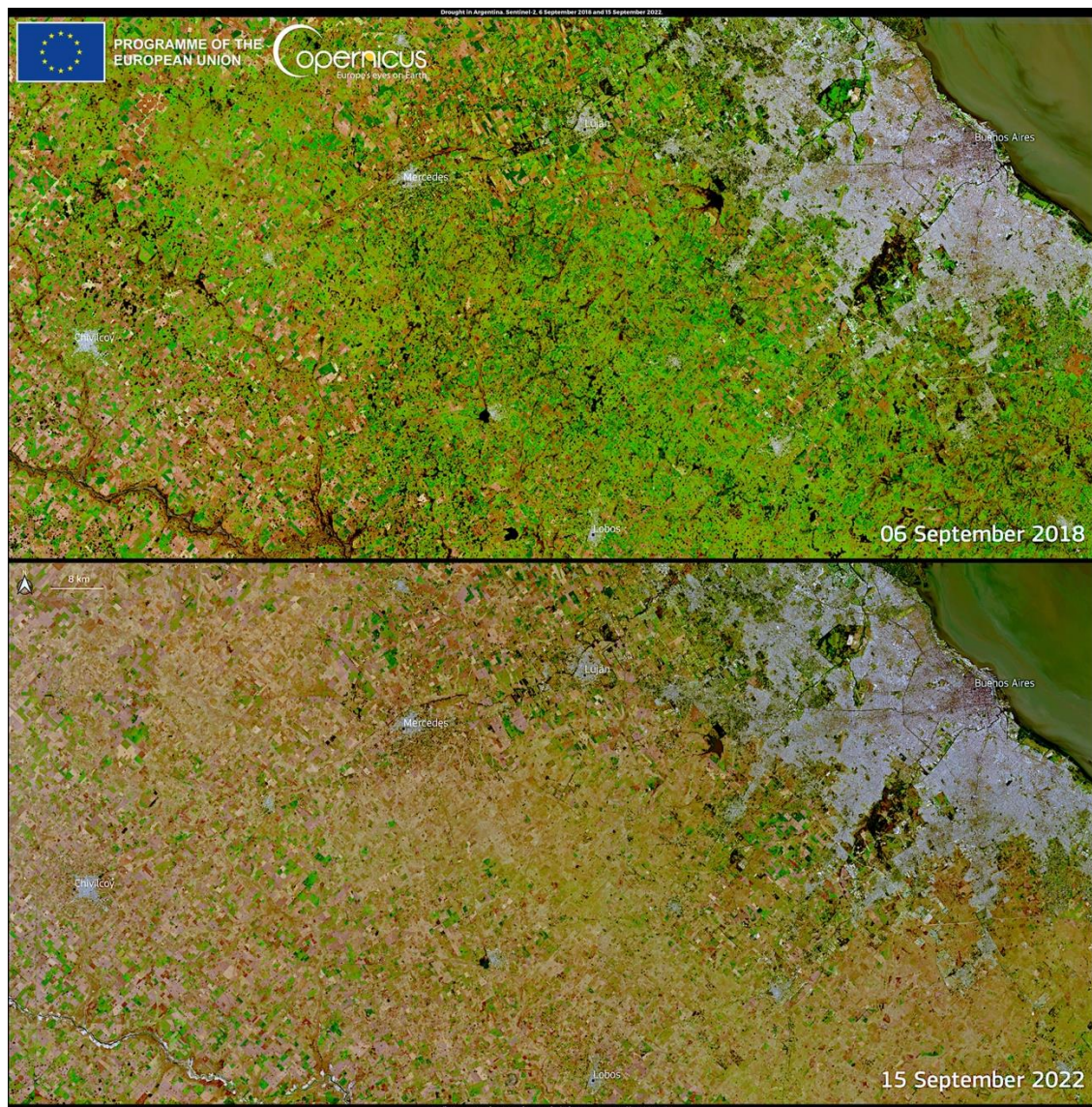


Figure 24. The consequences of dry conditions in the Pampas plains near the city of Buenos Aires (upper right corner of each image) are visible when comparing these two images acquired by Copernicus Sentinel-2 in September 2018 (above) and September 2022 (below). Source: European Union, Copernicus Sentinel-2 imagery.

In addition to reactive (declaration of emergencies) and proactive (development of early warning systems) governmental efforts to mitigate the impacts of droughts in the Argentine agricultural sector, individual decision-makers also have important roles in implementing multiple mitigation and recovery actions. A recent development intended to mitigate the agricultural impacts of precipitation deficits in Argentina was the adoption of late-sown maize. Maize was traditionally sown in late September and October and flowering occurred in late December or early January, when typically, there is less precipitation and high temperatures and solar radiation increase the evaporative demand (Bert et al., 2021). Instead, by delaying sowing to late November or early December, the yield-critical flowering period is shifted towards February, when the evaporative demand is lower. According to the Argentine Bolsa de Cereales (Grain Exchange), in 2021/22 the proportion of late-sowing maize (48% of total maize area) was almost equal to that of early sowed maize, suggesting a proactive action to prevent drought impacts.

4.4 Waterway Transportation

Naumann et al. (2021) showed that the dry event has been having important impacts on waterway transportation of goods in the basin. The Paraguay-Paraná Waterway (PPW, or “Hidrovía Paraná-Paraguay”) was highlighted as a major geopolitical component of the transportation system that provides ocean access to

land-locked South American countries (Paraguay and Bolivia). The 3400 km PPW joins southern Brazil to the Río de la Plata and the Atlantic Ocean. As many as 4500 barges, tugs and container ships sail up and down the PPW each year, carrying about 102 million tons of freight. The navigability of the PPW, however, is closely tied to the depth (and streamflow) of the Paraná and Paraguay rivers. Large seafaring ships (Panamax class, 36 ft draft) can only reach the Greater Rosario area in Santa Fe, Argentina (420 km of the waterway). Smaller ships (“handy max”, 28 ft draft) can get further north to the port of Santa Fe (590 km). North of Santa Fe, only inland barge traffic (10 ft draft) is possible.

The lack of rainfall, mainly in the upper part of the La Plata Basin, led to a considerable decrease in the flow of both the Paraguay (Figure 25) and Paraná rivers. By April 30, 2022, the Paraguay river level at Ladário reached 217 cm (20 cm below the long term mean of 237 cm). Ladário is the main port for export of iron ore from the Urucum massif (a mountain composed mostly by hematite) in the Brazilian state of Mato Grosso do Sul. This ore is loaded on barges with drafts of about 10 feet and transported down to Greater Rosario in Argentina or Nueva Palmira in Uruguay, where it is subsequently transferred to ocean-going vessels. Shipments of iron ore loaded at Ladário were about 2.0 and 1.67 million tons in 2020 and 2021, respectively. These shipments were much lower than during the three previous years, when transported volumes ranged between 3.3 and 3.7 M tons. Although some drivers not related to drought - the sale of the iron mines by the previous owner, the Vale Corporation - played a role in the sharply reduced shipments, difficulties due to reduced depths of the Paraguay River were an important driver (Treboux and Terré, 2022).

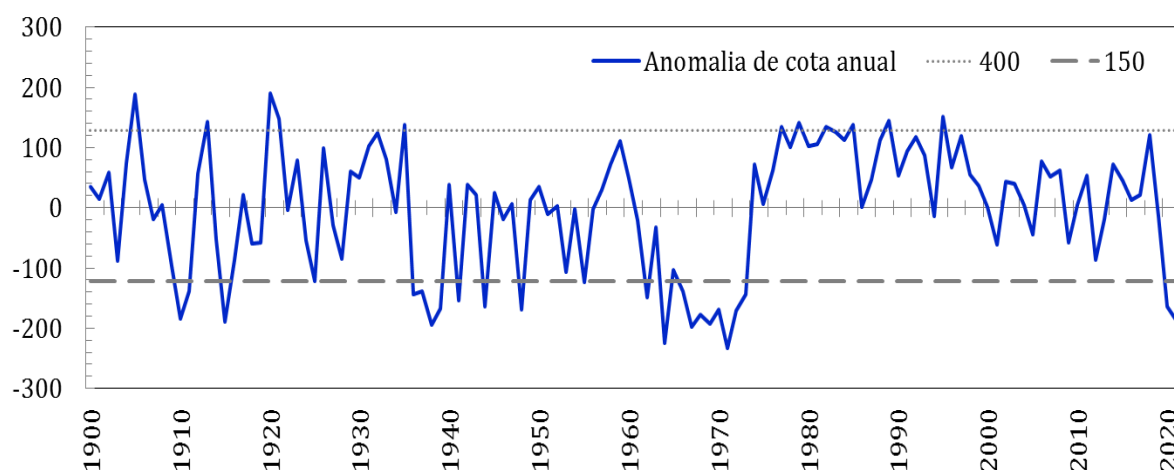


Figure 25. Anomalies (in cm) of the Upper Paraguay River level at Ladário. Base period is 1900-2020. Source: CEMADEN.

Argentina relies on the PPW to export 80% of its agricultural products, an important source of income for the country. Argentina and Brazil export a significant portion of its grain harvest along the Paraná. The PPW is a key waterway for the transport of grains and the situation is forcing exporters to consider using land routes. In recent years, many grain-bearing trade ships have had no choice but to lower their carrying capacities to prevent interference from the increasingly shallow riverbed. This has raised transportation prices which hinders economic growth.

The so-called “Greater Rosario” or “Up-River” area is a 70 km stretch on the Paraná River near the city of Rosario, Province of Santa Fe, Argentina, that encompasses the main soybean processing and export hub in the world, surpassing similar clusters in New Orleans (United States) and Santos (Brazil). The Greater Rosario cluster includes about 20 oilseed processing plants that account for about 80% of the Argentine crushing capacity; 12 of these plants have their own port terminal. In addition to Argentine soybeans, beans from Paraguay, Brazil and Bolivia are routinely transported to the greater Rosario cluster by barge. There, oilseeds can be processed into flour and oil or directly transferred to ocean-going vessels to be exported as beans.

To assess the likely impacts of Paraná River levels on the shipping activity near the Greater Rosario cluster, the temporal evolution of Paraná hydrometric levels near Rosario was shown in the earlier report on the LPB (see Naumann et al. 2021, Figure 18) for the period from December 2019 to August 2021. That figure is here updated (Figure 26) and now it shows the period January 2016 - June 2022. Additionally, it displays monthly median heights (calculated using the base period 1989-2020) to provide a useful reference for Paraná levels; the average monthly values are displayed as a dashed red line.

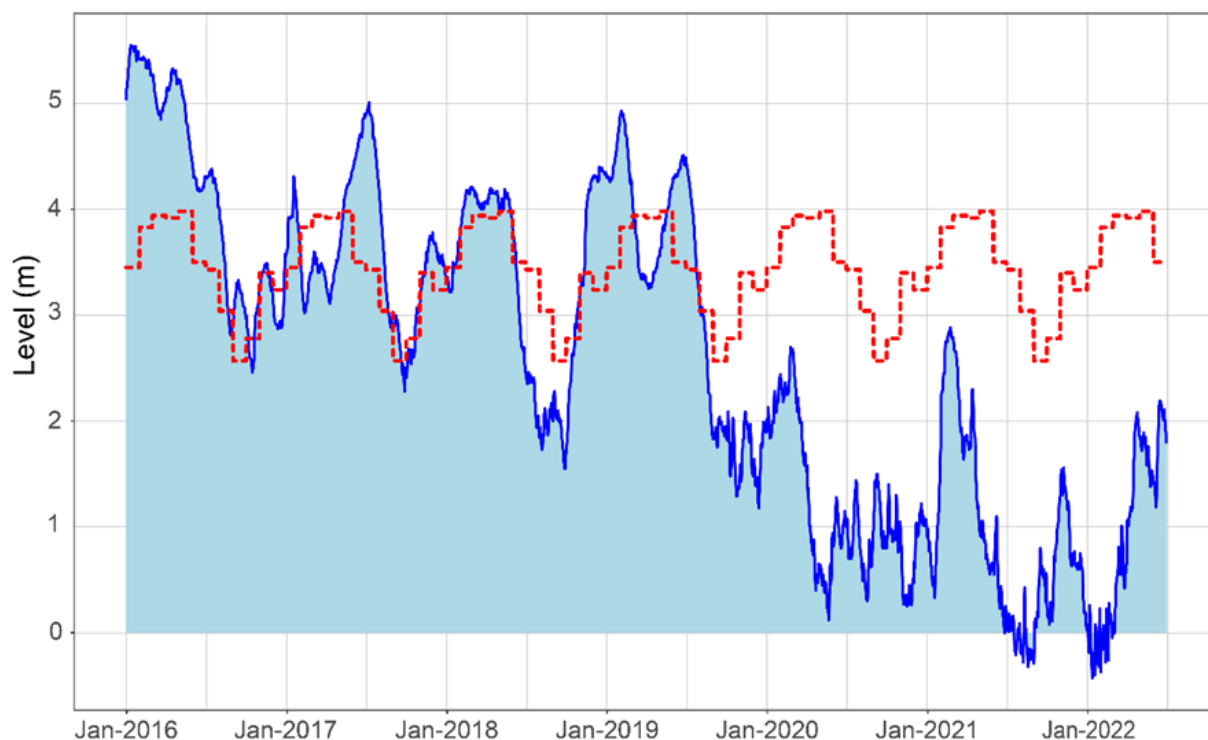


Figure 26. Hydrometric level of the Paraná River at the City of Rosario, Argentina, January 2016 to June 2022. The dashed red line indicates monthly median heights (calculated using the base period 1989-2020). Source: Instituto Nacional del Agua, Argentina.

As it was suggested by Paraná streamflow values (Figure 10), consistently low anomalies in Paraná hydrometric levels appeared in mid-2019. The higher levels that occurred in early 2020 remained about 2 meters below normal seasonal values, same as the values for early 2021. Values below the reference zero occurred in July-August 2021 and again in January-February 2022. After the extreme early-2022 lows, hydrometric levels started to rise in response to the already-described positive rainfall anomalies in the upper Plata basin during early 2022. By the end of the series (June 2022) hydrometric levels rose but remained about 2 m below normal levels.

The low PPW depth during the dry event forced ocean freighters leaving greater Rosario to decrease their normal loads. The lost freight capacity, in turn, resulted in higher costs per load. In mid-May 2020, PPW depth off greater Rosario was about 5 feet below its normal value, reducing the load of a Panamax by about 11,000 tons, or the load of about 370 trucks carrying 30 tons each. In addition to reducing ship loads, shallow waterway depths also raise navigational hazards, often restrict operations to daylight hours and increase the frequency of groundings. Furthermore, PPW low flows and depths also create problems on the landside of operations: slower navigation operations disrupt the overall flow of oilseeds and cereals.

A report prepared by the Rosario Trade Exchange (D'Angelo and Terré, 2022) suggests that the persistent dry event in the Paraná has had an impact on grain shipments. The report showed that the average load of ships leaving the Greater Rosario in the last quarter of 2021 was almost 11% lower than the one for the same period in 2020 – even though Paraná levels had similar anomalies at both times. At the same time, some of the shifts related to the low Paraná levels may be having lasting impacts. The report by D'Angelo and Terré also showed that the share of all grains, oil and sub products exported through Greater Rosario ports decreased from 78% in 2020 to 74% of the national total in 2021. In contrast, the deeper ocean port near Bahía Blanca (in the south of the Province of Buenos Aires) increased its 2021 share of national exports to a record high of 14%. The fact that the deeper southern ports are far away from the core Argentine production regions for soybean and maize implies additional costs to ship grains by land.

4.5 Hydroelectricity generation and other energy impacts and water supply for human consumption

Hydropower is the main source of renewable energy in South America, followed by biofuels. The LPB is one of the largest producers of hydroelectric power in the world (Rudnick et al., 2008). This region is endowed with 28% of the global water resources that, along with its topographical characteristics, contribute to the LPB high current and potential production of hydropower (Popescu et al., 2012). Dams and hydroelectric power plants in the LPB provide about 55% of the energy demand of countries in the basin. Hydropower plays an important role in the energy mix of Brazil, Uruguay, Argentina, Bolivia, and Paraguay (Table 1). Consequently, the high importance of HEP makes LPB countries highly dependent on water resource availability and drought conditions (Popescu, Brandimarte, and Peviani, 2014).

Table 1. Hydropower generation and share of total electrical generation in 2020. Source: International Renewable Energy Agency, IRENA, Statistical Profiles, <https://www.irena.org/Statistics/Statistical-Profiles>.

Country	Hydropower generation in 2020 (GWh)	Share of total national electrical generation in 2020 (%)
Brazil	396 382	64%
Bolivia	2 939	29%
Uruguay	4 094	30%
Argentina	29 685	20%
Paraguay	46 371	100%

The protracted drought and associated low river flows (Naumann et al 2021) continue to have a large impact on parts of the La Plata Basin. These low flows cause problems for energy production at the hydroelectric plants in the region. To explore the impacts, time series of electricity generation in various countries of the LPB have been collected from the websites of the national transmission system operators of Brazil⁽¹¹⁾, Uruguay⁽¹²⁾, Argentina⁽¹³⁾ and Bolivia⁽¹⁴⁾. Unfortunately, there is no data (yet) available for Paraguay. We analyze hydro-power generation because it is available for most of the countries under investigation. Reservoirs' levels and/or inflows - variables where the impact of drought would be more evident - are available only for a limited number of countries and hydro-power systems. We applied a 12-month rolling average to filter out the monthly variability due to dispatching.

Figure 27 shows that electricity production in the two binational power plants in the LPB - Yacyretá (Argentina-Paraguay) and Itaipú (Paraguay and Brazil) - have been drastically affected by the low levels of water. Itaipú shows a steady decrease since 2018 (upper left panel of Figure 27). A similar pattern is seen for Yacyretá (top panel of Figure 27), although the decrease in generation begins a little later than in Itaipú. In both cases, the

⁽¹¹⁾. http://www.ons.org.br/Paginas/resultados-da-operacao/historico-da-operacao/geracao_energia.aspx

⁽¹²⁾. <https://portal.ute.com.uy/institucional/ute/utei/fuentes-de-generacion>

⁽¹³⁾ <https://cammesaweb.cammesa.com/informe-sintesis-mensual/>

⁽¹⁴⁾. <https://www.cndc.bo/estadisticas/mensual.php>

decrease is consistent with the drought event. A negative trend can be observed also in Uruguay and in the binational power plant Salto Grande, a plant located on the Uruguay river on the border between Uruguay and Argentina. Data for Brazilian south (panel “BRA: Sul” in Figure 27) and southeast regions (panel “BRA: Sudeste/Centro-Oeste”) do not show a clear trend but in general a low generation, with the exception of the June-July 2022 for Sul and last winter for the southeast regions. Uruguay and the Mesopotamia region of Argentina show a decrease in generation possibly associated with low flows in the Uruguay River, although both countries exhibit an increase in the last portion of the series (late 2021). Other parts of Argentina and Bolivia do not seem to show consistent decreases in recent years.

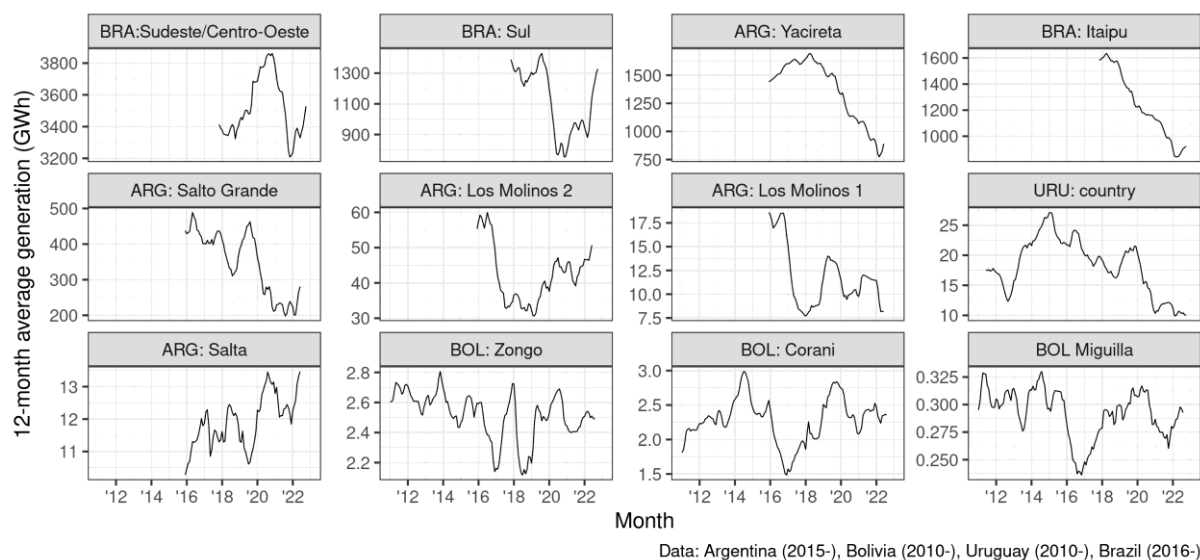


Figure 27. Monthly hydropower generation for the previous 12 months. Source: websites of the national transmission system operators for countries shown (data updated 01/10/2022 – see footnotes at page 36).

The drop in hydropower productivity has not yet led to an “energy crisis” according to the Instituto Nacional del Agua (INA) but has led countries to turn to less sustainable energy sources such as thermoelectric, which utilizes fossil fuels.

5 Knowing and doing better: ongoing efforts on regional drought monitoring

This section presents a non-exhaustive review of drought monitoring systems, research projects and institutional efforts focus to cope with drought in the region.

5.1 Drought monitoring in Argentina

No coordinated drought information system (DIS) exists in Argentina. Nevertheless, two promising developments have recently happened: one at the national level, and another one with a broader regional scope. At the national level, Argentina has created the Sistema Nacional para la Reducción del Riesgo de Desastres y la Protección Civil (SINAGIR, <https://oavv.segemar.gob.ar/sinagir/>), an institutional framework for the coordination and planning of a broad spectrum of geophysical risks. Within the SINAGIR framework, a network was established among science and technology institutions linked to the management of various climate and geophysical risks; this network is called GIRCYT (Spanish acronym). GIRCYT facilitated the design of an “Interinstitutional Protocol to Manage Information about Meteorological and Agricultural Droughts” in Argentina. The protocol motivated the formation of a Drought Monitoring Roundtable (DMR) that is playing a crucial role in coordinating the separate, sometimes overlapping efforts of governmental and academic institutions involved on drought.

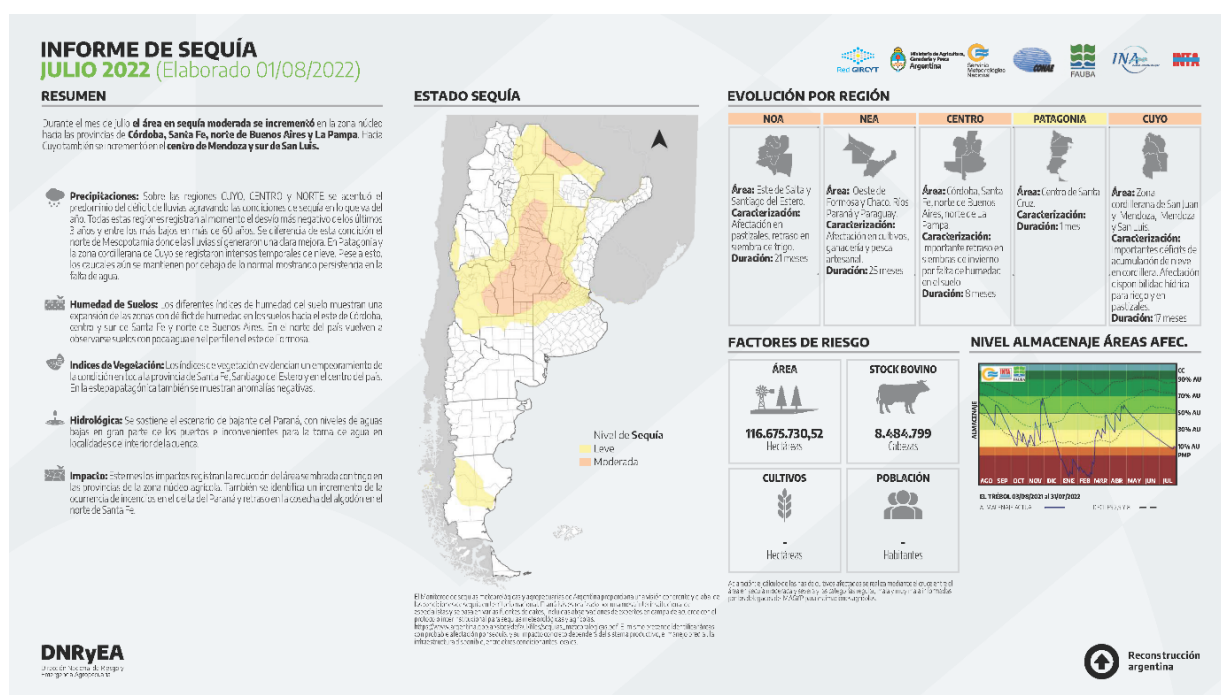


Figure 28. Example of a drought status report produced by Argentine Drought Monitoring Roundtable, July 2022. The map in the report shows moderate drought in the Pampas of central-eastern Argentina. Source: Mesa Nacional de Monitoreo de Sequías, Argentina⁽¹⁵⁾.

The DMR meets regularly to monitor ongoing and forecasted drought conditions across Argentina. This information, however, is provided mainly to governmental agencies; no broad public dissemination takes place yet. Upcoming governmental programs seek a more proactive mitigation of the impacts of droughts and other climatic hazards in Argentina. For example, the project GIRSAR (Gestión Integral de los Riesgos en el Sector Agroindustrial Rural) is currently in the early onset phase. Financed through a loan from the International Bank for Reconstruction and Development, GIRSAR will strengthen capabilities needed to manage drought risks in Argentina, including the production and dissemination of agro-climatic information. The project also seeks to

⁽¹⁵⁾.

https://www.magyp.gob.ar/sitio/areas/d_edasequia/_archivos//220000_Informes%202022/220700_Informe%20de%20Sequ%C3%ADa%20-%20Julio%202022.pdf

promote the development and adoption of financial instruments to transfer climatic and market risks in agricultural production. At the same time, the Argentine Agricultural Research Institute (INTA) and the academic institutions continue to develop good agronomic practices to reduce risks and stabilize yields as well as income. A recent development is the increasing role of public-private partnerships in identifying pathways towards resilient agricultural systems: an example is the joint development of HB4 technology to produce drought-tolerant transgenic soybean and wheat.

5.2 Drought Monitoring in Brazil

5.2.1 Drought Monitor of the National Water Agency

In its newest phase, the Drought Monitor has the National Water Agency (ANA) as the central institution of the process. ANA is responsible for the coordination at the federal level and for the articulation with all participating States, as well as its ongoing expansion to other ones. Monthly information about drought is made available up to the previous month, with indicators that reflect the short term (last 3, 4 and 6 months) and long term (last 12, 18 and 24 months), indicating the evolution of the drought in the region.

Figure 29 shows a recent Drought Monitor Map (July 2022) and a description of the drought status in participating Brazilian states.

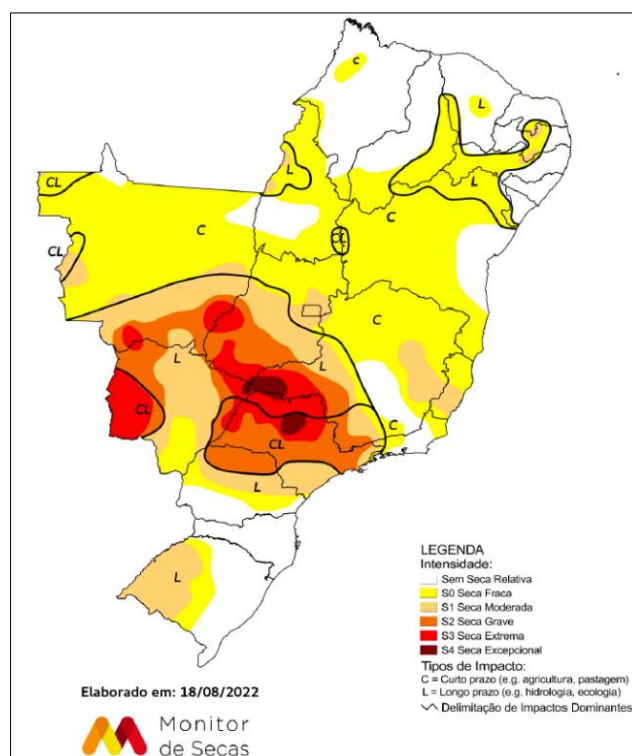


Figure 29. Brazilian Drought Monitor map for July 2022. In the Southeast Region, due to negative rainfall anomalies and worsening indicators, there was an increase in the area with weak drought (S0) in the north of Minas Gerais and Rio de Janeiro. Drought worsened in the states of Espírito Santo and east-central Minas Gerais, going from weak (S0) to moderate (S1) conditions. Source: <https://monitordesecas.ana.gov.br>

The development of a Drought Monitor in Brazil is aligned with the most recent discussions and other initiatives at both national and international levels. The Drought Monitor aims to integrate the technical and scientific knowledge that already exists in different States and federal institutions to reach a common understanding of the drought conditions, such as severity, spatial and temporal evolution, and impacts on different sectors. This work responds to a historical need to improving the monitoring and management of droughts in Brazil and represents the first step towards a new approach - from emergency and reactive management to proactive preparation and management.

In addition, ANA supports some of the Brazilian Hydrologic Warning Systems in compliance with its legal duties to plan and promote prevention and mitigation of droughts and flood. The ANA Situation Room also issues

announcements when a critical hydrologic event is detected (both flood and drought) in any monitored river or reservoir. This communication happens through reports, issued by the Situation Room, for more information see <https://monitordesecas.ana.gov.br/o-monitor-de-secas>.

5.2.2 Drought Monitoring System of CEMADEN

Drought monitoring at the Brazilian National Centre for Monitoring and Early Warning of Natural Disasters (CEMADEN) is focused mainly on the expected impacts on agriculture (agricultural drought) and water resources (hydrological drought). CEMADEN's drought monitoring efforts began in 2013 in response to the severe and extended drought that started in 2012 in northeast Brazil. The federal government asked CEMADEN to support the identification of municipalities affected by drought to subsidize emergency support for the municipalities; drought monitoring by CEMADEN has continued since then. Specifically for monitoring meteorological and agricultural drought, the Centre has developed an Integrated Drought Index, which includes precipitation deficit (SPI), soil moisture from CEMADEN's observational network and estimated from satellite, and two drought indexes based on remote sensing (Vegetation Water Supply Index and Vegetation Health Index). In addition to conducting drought and impact monitoring, as a research centre of the Ministry of Science, Technology, and Innovation (MCTI), CEMADEN aims to generate scientific and technological knowledge on hazards, processes, and vulnerabilities associated with droughts and their impacts, to support society and decision-makers.

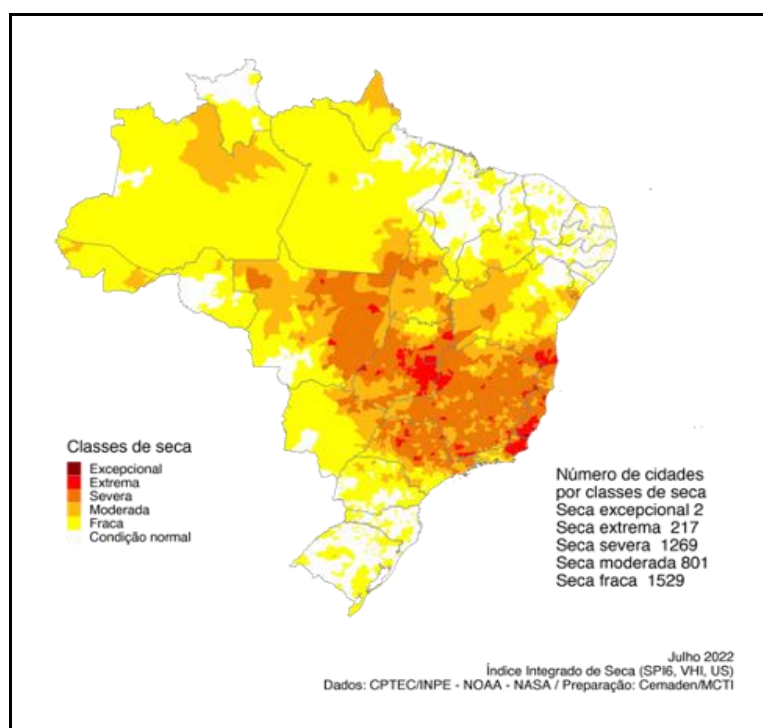


Figure 30. Integrated drought index for July 2022 considering the 6-month temporal scale indicating drought severity over Brazilian municipalities. Source: CEMADEN.

Percentage of agricultural area potentially affected by drought
(by rural establishment size) – August 2022

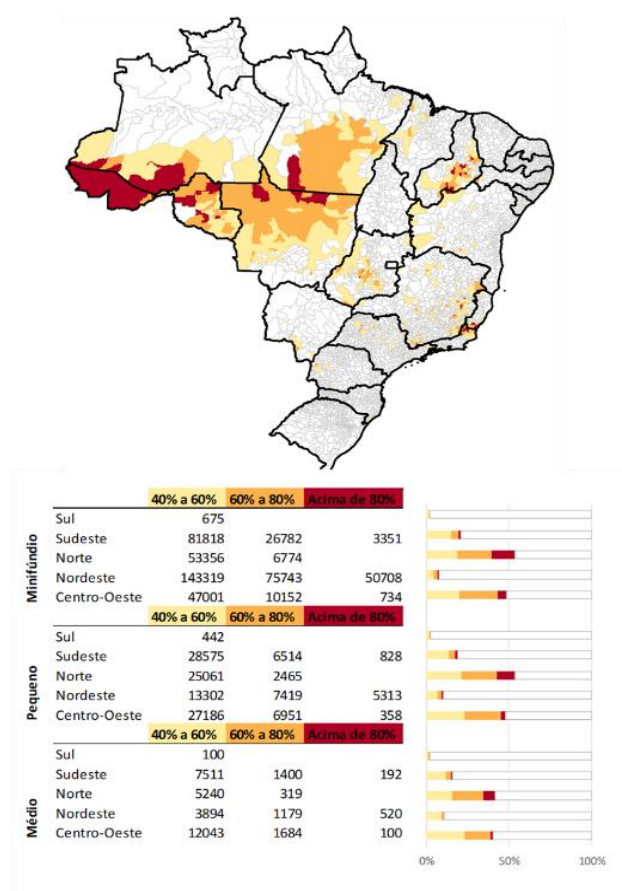


Figure 31. Using agricultural drought indicators filtered by an agricultural land mask, CEMADEN estimates the percentage of agricultural area at the municipality level affected by drought. It is also possible to have a diagnosis of the sizes of the most affected rural establishments. The figure shows the conditions for August 2022. Source: CEMADEN.

CEMADEN also monitors and evaluates the phenological cycle of the main crops of the region (maize and beans) using a remote sensing-based index with a spatial resolution of 250 meters. This specific monitoring aims to meet the requirements established in Presidential Decree No. 8472 for the Agricultural Yield Guarantee Programme (Garantia Safra Program, GS) of the Ministry of Agriculture, Livestock and Supply (MAPA), which is related to the identification of municipalities affected by drought. The GS Program aims to guarantee a minimum allowance to subsistence agriculture farmers when affected by drought or rainfall in excess.

In the context of disaster risk related to drought, CEMADEN also produces monthly maps of drought risk focused on smallholder agriculture. For this, socioeconomic variables tied to vulnerability (V) and adaptive capacity (AC) are combined with hazard information organized on a municipal scale ⁽¹⁶⁾.

Since 2014, due to the intense drought in the Southeast, CEMADEN has established a monitoring system for the Cantareira System (Figure 32), the largest water supply system for the Metropolitan Region of São Paulo, which between 2014 and 2016 suffered the worst water crisis, getting so bad as to make use of the dead volume (Nobre et al., 2016, Deusdará-Leal et al., 2020). CEMADEN monitors long-term droughts (time scale of 12-months to 36-months) in several important basins for water supply and hydropower generation (Cuartas et al., 2022). For some basins, CEMADEN also provides discharge and reservoir levels forecast for up to 10 days and projections for 3 to 12 months, based on precipitation scenarios.

⁽¹⁶⁾ (<https://www.gov.br/cemaden/pt-br/assuntos/monitoramento/seca-na-agricultura-familiar/risco-de-seca-na-agricultura-familiar-maio-2022>)

Cantareira System: monitoring & projections

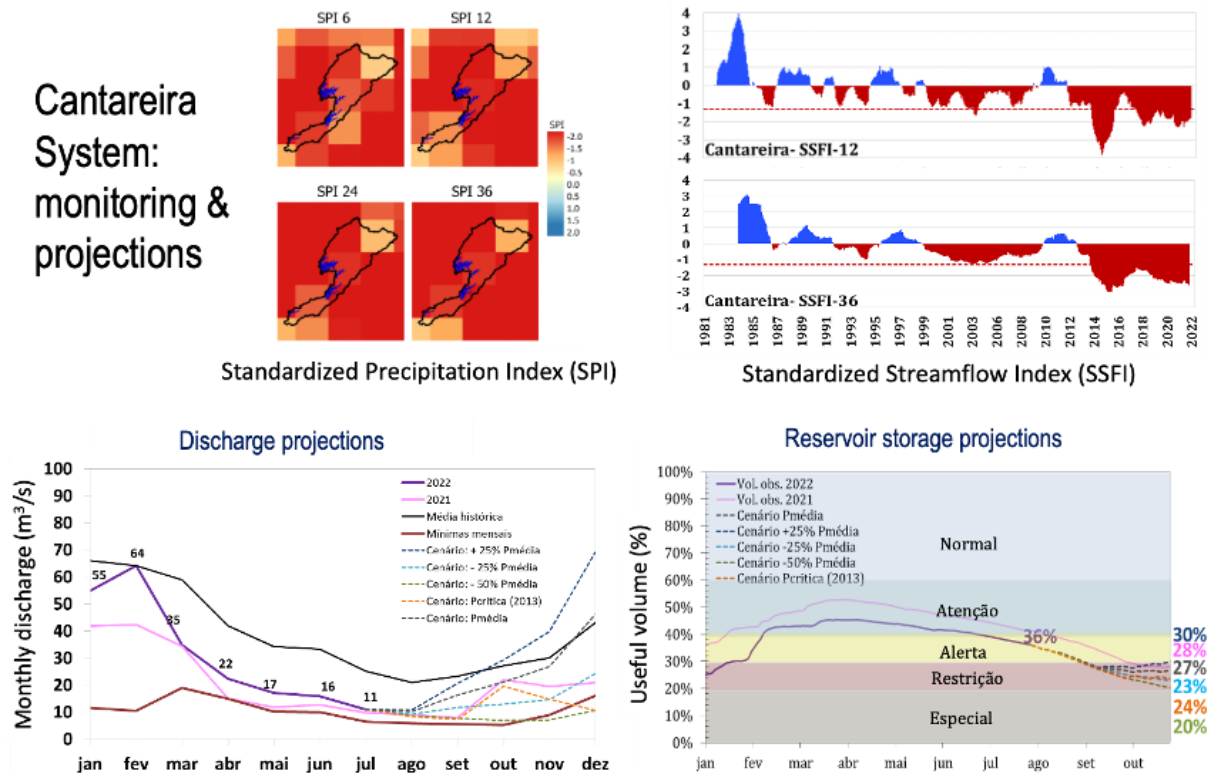


Figure 32. Example of drought monitoring and projections of the Cantareira system, the largest water supply system for the Metropolitan Region of São Paulo. Upper left: SPI values at time scales of 6 to 36 months show the long-term drought conditions for July 2022. Upper right: time series of SSFI at 12-time and 36-time scale show the critical hydrological situation (hydrological drought) since 2014. Lower left and right: The projected inflow and reservoir level obtained from hydrological modelling. Source: CEMADEN.

This information is provided at regular meetings of the Monitoring Rooms for several basins and regions, coordinated by the National Water and Sanitation Agency (ANA), and formed by the Electric System Operator (ONS, IBAMA) basin committees and state institutions. Online reports are available on the CEMADEN website (<https://www.gov.br/cemaden/pt-br/assuntos/monitoramento>).

5.3 Drought monitoring in Bolivia

The Bolivian Drought Monitor (<http://monitorsequias.senamhi.gob.bo>) is a platform for monitoring and disseminating drought conditions throughout the Bolivian territory. The Monitor is an important component of the National Early Warning System for Disasters (SNATD) regulated by the Risk Management Law (Law 602). The Bolivian Drought Monitor is a joint effort of four different Bolivian national institutions: the Ministry of Environment and Water (MMAyA), the National Service of Meteorology and Hydrology (SENAMHI), the Vice-ministry of Civil Defence (VIDECI), dependent from the Ministry of Defence, and the Ministry of Rural Development and Lands (MDRyT). These four institutions provide multi-sectoral analyses of drought conditions (weather and climatic analysis, impact on water resources, agricultural sector, and humanitarian field) and generate monthly information for the public on the severity, space-time evolution and the expected impacts on different sectors.

Given the limited availability of in-situ meteorological information in Bolivia, the Drought Monitor relies strongly on a large variety of multi-source satellite products. These latter are used to provide monthly maps of 17 indexes covering meteorological, hydrological, and agricultural droughts for different aggregation periods (from 1 to 12 months).

A compound drought index based on the combination of four indexes (SPEI-3, SSMI-2, VHI-1 and FAPAR-1) was chosen to provide a synthesis of the hazard conditions likely to generate impacts. As depicted in Figure 33,

during the first part of 2022, the combined index shows increasingly critical conditions in the south-eastern part of the country partially belonging to the La Plata Basin (Chiquitania and Chaco), with 20% of the territory currently affected by severe drought in El Chaco.

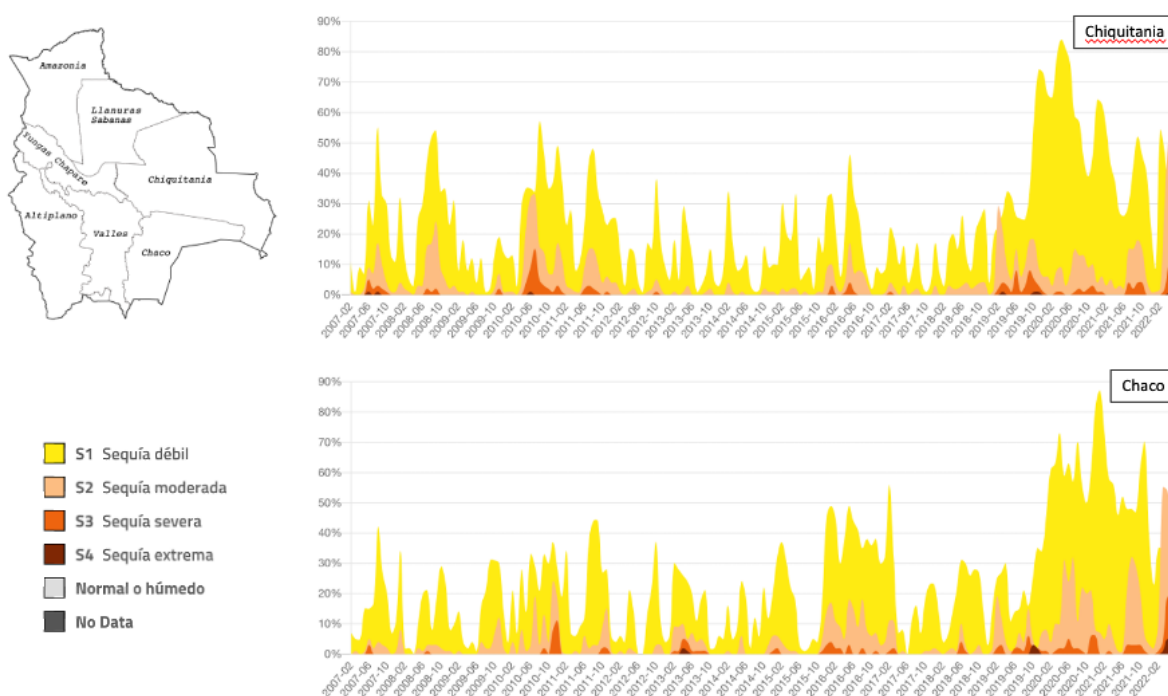


Figure 33. Time series of the areas under different drought conditions in two regions in the eastern part of Bolivia that are part of the La Plata Basin: Chiquitania (above) and Chaco (below); see the inset map on the left for the location of these regions. An increase in the areas under weak (S1) and moderate (S2) drought conditions can be seen starting in mid-2021. Source: Bolivian Drought Monitor (<http://monitoresequias.senamhi.gob.bo>)

5.4 Drought monitoring in Paraguay

The Direction of Meteorology and Hydrology (DMH) under the Directorate of Civil Aviation (DINAC) continuously monitors weather and climate and issues a monthly weather bulletin and a seasonal weather outlook bulletin. Although DMH does not carry out specific drought monitoring on a systematic basis, systematic climate monitoring allows DMH to report on the occurrence and evolution of drought phenomena, as well as to forecast the possible occurrence of drought. In the past, DMH has conducted specific studies for particular events, for example by analysing indices such as SPI and SPEI. DMH currently uses the products and information provided by the SISSA project of the Regional Climate Centre for Southern South America for drought monitoring.

5.5 Drought monitoring in Uruguay

There are multiple institutions involved in drought monitoring in Uruguay. The Instituto Uruguayo de Meteorología (INUMET, www.inumet.uy) is the national meteorological agency. INUMET routinely produces SPI maps on several temporal scales (an example is shown in Figure 34 left panel). Because of the high importance of crop and cattle production to the economy of Uruguay, another important source of drought information is the national agricultural research institute (Instituto Nacional de Investigación Agropecuaria, INIA, www.inia.uy), particularly its Unidad de Agroclima y Sistemas de información (GRAS, <http://www.inia.uy/gras>). INUMET and INIA/GRAS jointly produce a country-wide soil water balance (Figure 34 centre panel). INIA/GRAS also monitors other variables tied to drought, such as NDVI and its anomalies (Figure 34 right panel) or APAR (Absorbed Photosynthetically Active Radiation).

SPI-3 - December 2022

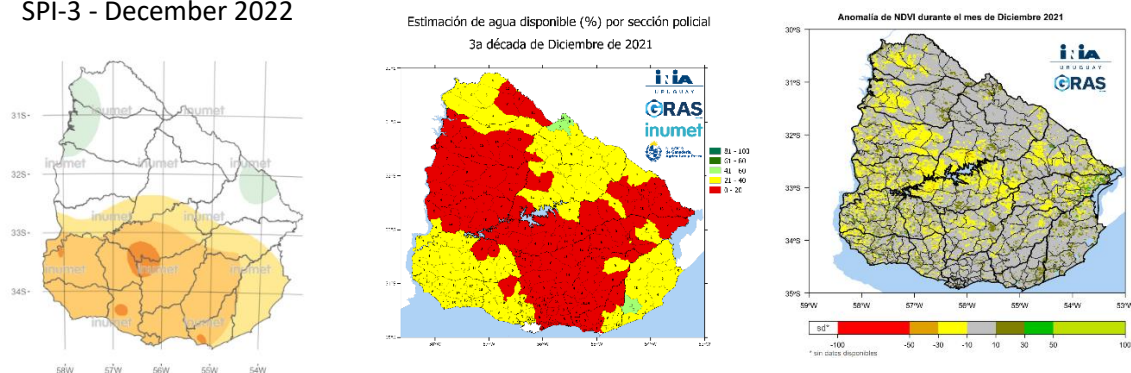


Figure 34. Left: INUMET SPI-3 map for Uruguay, September 2022 derived from data at 18 in-situ meteorological stations. Centre: Soil water balance (INIA/GRAS and INUMET) for the third decade of December 2021, showing country-wide moisture deficits. Right: NDVI anomalies in December 2021 produced by INIA/GRAS.

5.6 Regional drought monitoring: Sistema de Información sobre Sequías para el sur de Sudamérica - SISSA

A promising development at the regional level is the Drought Information System for southern South America (or SISSA, for its Spanish acronym) that was launched in 2019. The SISSA (<https://sisa.crc-sas.org/>) is a project operating under the umbrella of WMO's Regional Climate Centre for southern South America (RCC-SSA), a six-nation collaboration to produce and disseminate timely, relevant and actionable climate information and services to support decision making in societal sectors sensitive to climate variability and change. Both the RCC-SSA and SISSA encompass six countries in southern South America: Argentina, Bolivia, Brazil (south of 10°S), Chile, Paraguay, and Uruguay.

In addition to disseminating drought monitoring products derived from in situ and satellite data, SISSA aims to contribute to reduce the considerable economic, social, and environmental impacts of drought on agricultural production, hydroelectric generation, and waterway transportation in southern South America together with improvements in: (i) regional institutional capacities, (ii) planning and preparation, and (iii) risk management governance

The main institutions that collaborate in SISSA are the National Meteorological and Hydrological Services of the six countries of the CRC-SAS. Nevertheless, SISSA also seeks to work actively with government natural resource management and disaster risk management institutions and with governmental and academic research institutions in climatic, agronomic, hydrological, social, environmental, and engineering sciences. Support for SISSA activities is provided by the Regional Public Goods program of the Inter-American Development Bank (IADB) and by the EUROCLIMA+ program funded by the European Union through the Spanish Agency for International Cooperation (AECID).

6 Conclusions

A multi-year drought has been affecting the La Plata Basin since mid-2019. The lack of rainfall, mainly in the upper part of the basin, has led to a considerable decrease in the flow of the Paraguay and Paraná rivers. A detailed description of the onset, evolution and related impacts of this event has been given in Naumann et al., 2021.

As of August 2022, soil moisture anomaly appears to be generally near normal conditions or not extensively dryer than normal. An exception is the central part of the La Plata Basin in the Brazilian Mato Grosso do Sul state, having wetter-than-normal soil conditions. Similarly, FAPAR generally shows close-to-normal or lower-than-normal values, except for a wide region including north-eastern Argentina, southern Brazil, and Uruguay.

Seasonal models consistently forecast negative precipitation anomalies over the LPB, partially as a response to the negative sea surface temperatures (SST) anomalies in the tropical pacific associated with La Niña condition. There are high chances that La Niña conditions will prevail for another season, and we may have a third consecutive spring and summer with La Niña conditions. Similarly, multi-annual to decadal modes of climate variability (i.e., AMO, PDO) are in a phase that favours drought in the LPB.

Due to its prolonged duration and severity, this drought has already had numerous impacts on different socio-economic sectors and has also severely affected ecosystems. These include forest fires, reduced agricultural yields, reduced river transport on the Paraguay and Paraná rivers, and a significant reduction in hydropower production. Regional impacts on ecosystems and biodiversity are severe, especially acute in the Pantanal, one of the largest wetlands in the Americas.

References

- Agrositio, 'Sequía e incendios se agravan en el norte del país', 2022.
<http://www.agrositio.com.ar/noticia/221749-sequia-e-incendios-se-agravan-en-el-norte-del-pais>.
- Ambito, 'Alertan sobre bacterias en el río Paraná, y recomiendan evitar bañarse en las orillas', 2022.
<https://www.ambito.com/informacion-general/parana/alertan-bacterias-el-rio-y-recomiendan-evitar-banarse-las-orillas-n5367897>.
- Anderson, M.C., C.A. Zolin, P.C. Sentelhas, C.R. Hain, K. Semmens, M. Tugrul Yilmaz, F. Gao, J.A. Otkin, and R. Tetrault, 'The Evaporative Stress Index as an Indicator of Agricultural Drought in Brazil: An Assessment Based on Crop Yield Impacts', *Remote Sensing of Environment*, Vol. 174, March 1, 2016, pp. 82–99.
- Arias, L., 'Corrientes tras los incendios: ¿Cómo están hoy los Esteros del Iberá?', *A24*, 2022.
<https://www.a24.com/actualidad/corrientes-los-incendios-como-estan-hoy-los-esteros-del-ibera-n1004178>.
- Barbosa, P., D. Magni, J. Vogt, J. Spinoni, D. Masante, A. De Jager, G. Naumann, et al., *Droughts in Europe and Worldwide 2019-2020*, Publications Office of the European Union, Luxembourg, 2021.
- Cammalleri, C., P. Barbosa, and J.V. Vogt, 'Evaluating Simulated Daily Discharge for Operational Hydrological Drought Monitoring in the Global Drought Observatory (GDO)', *Hydrological Sciences Journal*, Vol. 65, No. 8, 2020, pp. 1316–1325.
- Cammalleri, C., C. Arias-Muñoz, P. Barbosa, A. de Jager, D. Magni, D. Masante, M. Mazzeschi, et al., 'A Revision of the Combined Drought Indicator (CDI) Used in the European Drought Observatory (EDO)', *Natural Hazards and Earth System Sciences*, Vol. 21, No. 2, February 2, 2021, pp. 481–495.
- Cammalleri, C., P. Barbosa, and J.V. Vogt, 'Analysing the Relationship between Multiple-Timescale SPI and GRACE Terrestrial Water Storage in the Framework of Drought Monitoring', *Water*, Vol. 11, No. 8, 2019, p. 1672.
- Cammalleri, C., J. Vogt, and P. Salamon, 'Development of an Operational Low-Flow Index for Hydrological Drought Monitoring over Europe', *Hydrological Sciences Journal*, Vol. 62, No. 3, February 17, 2017, pp. 346–358.
- Cammalleri, C., J.V. Vogt, B. Bisselink, and A. de Roo, 'Comparing Soil Moisture Anomalies from Multiple Independent Sources over Different Regions across the Globe', *Hydrology and Earth System Sciences*, Vol. 21, No. 12, 2017, pp. 6329–6343.
- Carrao, H., G. Naumann, and P. Barbosa, 'Mapping Global Patterns of Drought Risk: An Empirical Framework Based on Sub-National Estimates of Hazard, Exposure and Vulnerability', *Global Environmental Change*, Vol. 39, 2016, pp. 108–124.
- Centenera, M., 'Los incendios arrasan casi el 10% de la provincia argentina de Corrientes', *El País*, February 22, 2022. <https://elpais.com/internacional/2022-02-22/los-incendios-arrasan-casi-el-10-de-la-provincia-argentina-de-corrientes.html>.
- Cuartas, L.A., A.P.M. do A. Cunha, J.A. Alves, L.M.P. Parra, K. Deusdará-Leal, L.C.O. Costa, R.D. Molina, et al., 'Recent Hydrological Droughts in Brazil and Their Impact on Hydropower Generation', *Water*, Vol. 14, No. 4, January 2022, p. 601.
- Cuevas, S.M., 'Cianobacterias: cómo cuidarse de las algas tóxicas y meterse en el agua de forma segura', *infobae*, 2022. <https://www.infobae.com/salud/ciencia/2022/02/07/cianobacterias-como-cuidarse-de-las-algas-toxicas-y-meterse-en-el-agua-de-forma-segura/>.
- D'Angelo, G., and E. Terré, 'Por la bajante, la participación del Gran Rosario en los embarques argentinos es la más baja en 23 años', *Bolsa de Comercio de Rosario*, January 7, 2022.
<http://www.bcr.com.ar/es/mercados/investigacion-y-desarrollo/informativo-semanal/noticias-informativo-semanal/por-la-0>.
- European and Global Drought Observatories, 'GDO Fraction of Absorbed Photosynthetically Active Radiation (FAPAR) Anomaly (MODIS) (Version 1.3.1)', April 30, 2021.
- Funk, C., P. Peterson, M. Landsfeld, D. Pedreros, J. Verdin, S. Shukla, G. Husak, J. Rowland, L. Harrison, and A. Hoell, 'The Climate Hazards Infrared Precipitation with Stations—a New Environmental Record for Monitoring Extremes', *Scientific Data*, Vol. 2, No. 1, 2015, pp. 1–21.
- Gobron, N., B. Pinty, F. Mélin, M. Taberner, M.M. Verstraete, A. Belward, T. Laverigne, and J.-L. Widlowski, 'The State of Vegetation in Europe Following the 2003 Drought', *International Journal of Remote Sensing*, Vol. 26, No. 9, 2005, pp. 2013–2020.
- Gomes, M.S., I.F. de A. Cavalcanti, and G.V. Müller, '2019/2020 Drought Impacts on South America and Atmospheric and Oceanic Influences', *Weather and Climate Extremes*, Vol. 34, December 1, 2021, p. 100404.

- Grimson, R., N. Montroull, R. Saurral, P. Vasquez, and I. Camilloni, 'Hydrological Modelling of the Iberá Wetlands in Southeastern South America', *Journal of Hydrology*, Vol. 503, October 30, 2013, pp. 47–54.
- Hermanson, L., D. Smith, M. Seabrook, R. Bilbao, F. Doblas-Reyes, E. Tourigny, V. Lapin, et al., 'WMO Global Annual to Decadal Climate Update: A Prediction for 2021–25', *Bulletin of the American Meteorological Society*, Vol. 103, No. 4, April 1, 2022, pp. E1117–E1129.
- Hiba, J., 'Tragedia ecológica en Corrientes: los incendios llegaron a los Esteros del Iberá y amenazan su amplia biodiversidad', *LA NACION*, February 15, 2022. <https://www.lanacion.com.ar/sociedad/tragedia-ecologica-en-corrientes-los-incendios-llegaron-a-los-esteros-del-ibera-y-amenazan-su-amplia-nid15022022/>.
- Knijff, J.M.V.D., J. Younis, and A.P.J.D. Roo, 'LISFLOOD: A GIS-based Distributed Model for River Basin Scale Water Balance and Flood Simulation', *International Journal of Geographical Information Science*, Vol. 24, No. 2, February 1, 2010, pp. 189–212.
- Kooperberg, C., and C.J. Stone, 'A Study of Logspline Density Estimation', *Computational Statistics & Data Analysis*, Vol. 12, No. 3, 1991, pp. 327–347.
- Libonati, R., J.L. Geirinhas, P.S. Silva, A. Russo, J.A. Rodrigues, L.B.C. Belém, J. Nogueira, et al., 'Assessing the Role of Compound Drought and Heatwave Events on Unprecedented 2020 Wildfires in the Pantanal', *Environmental Research Letters*, Vol. 17, No. 1, January 2022, p. 015005.
- Liu, Y.Y., W.A. Dorigo, R.M. Parinussa, R.A.M. de Jeu, W. Wagner, M.F. McCabe, J.P. Evans, and A.I.J.M. van Dijk, 'Trend-Preserving Blending of Passive and Active Microwave Soil Moisture Retrievals', *Remote Sensing of Environment*, Vol. 123, August 1, 2012, pp. 280–297.
- Marengo, J.A., T. Ambrizzi, N. Barreto, A.P. Cunha, A.M. Ramos, M. Skansi, J.M. Carpio, and R. Salinas, 'The Heat Wave of October 2020 in Central South America', *International Journal of Climatology*, 2021.
- Marengo, J.A., A.P. Cunha, L.A. Cuartas, K.R. Deusdará Leal, E. Broedel, M.E. Seluchi, C.M. Michelin, C.F. De Praga Baião, E. Chuchón Ângulo, and E.K. Almeida, 'Extreme Drought in the Brazilian Pantanal in 2019–2020: Characterization, Causes, and Impacts', *Frontiers in Water*, Vol. 3, 2021, p. 13.
- Mata, J.C., R. Buitenwerf, and J.-C. Svenning, 'Enhancing Monitoring of Rewilding Progress through Wildlife Tracking and Remote Sensing', *PLOS ONE*, Vol. 16, No. 7, July 9, 2021, p. e0253148.
- McKee, T.B., N.J. Doesken, and J. Kleist, 'The Relationship of Drought Frequency and Duration to Time Scales', *Proceedings of the 8th Conference on Applied Climatology*, Vol. 17, American Meteorological Society Boston, MA, 1993, pp. 179–183.
- Meehl, G.A., J.H. Richter, H. Teng, A. Capotondi, K. Cobb, F. Doblas-Reyes, M.G. Donat, M.H. England, J.C. Fyfe, and W. Han, 'Initialized Earth System Prediction from Subseasonal to Decadal Timescales', *Nature Reviews Earth & Environment*, Vol. 2, No. 5, 2021, pp. 340–357.
- Naumann, G., G. Podesta, J. Marengo, J. Luterbacher, D. Bavera, C. Arias-Muñoz, F.B.P. Marinho, et al., 'The 2019–2021 Extreme Drought Episode in La Plata Basin', *JRC Publications Repository*, October 13, 2021. <https://publications.jrc.ec.europa.eu/repository/handle/JRC126508>.
- Noticias Ambientales, 'Aparecieron cianobacterias en diferentes lugares de la cuenca del río Paraná', *Noticias Ambientales*, December 7, 2022. <https://noticiasambientales.com/ciencia/aparecieron-cianobacterias-en-diferentes-lugares-de-la-cuenca-del-rio-parana/>.
- , 'El Paraná se queda sin agua: dos años de sequía ponen en jaque a una de las mayores cuencas sudamericanas', *Noticias ambientales*, August 6, 2021. <https://es.mongabay.com/2021/08/parana-el-plata-cuenca-rios-sequia-argentina-brasil-paraguay/>.
- OMEGA, 'Las Áreas Identificadas En Sequía Severa Incluyen Centro y Sur de Misiones, Este de Formosa y Chaco, Toda La Provincia de Corrientes y Una Porción Norte de Entre Ríos. Report to the National Commission of Agricultural Emergencies and Disasters Presented on 17 February 2022', https://www.magyp.gob.ar/sitio/areas/d_ed/sequia/_archivos//220000_Informes%202022/220100_Informe%20de%20Sequ%C3%ADa%20-%20Enero%202022.pdf, 2022.
- Parana hacia el Mundo, 'Harán un mapeo de cianobacterias en el río Paraná', *Paraná hacia el Mundo*, December 15, 2022. <https://paranahaciaelmundo.com/haran-un-mapeo-de-cianobacterias-en-el-rio-parana/>.
- Popescu, I., L. Brandimarte, M.S.U. Perera, and M. Peviani, 'Assessing Residual Hydropower Potential of the La Plata Basin Accounting for Future User Demands', *Hydrology and Earth System Sciences*, Vol. 16, No. 8, 2012, pp. 2813–2823.
- Popescu, I., L. Brandimarte, and M. Peviani, 'Effects of Climate Change over Energy Production in La Plata Basin', *International Journal of River Basin Management*, Vol. 12, No. 4, 2014, pp. 319–327.

- Rudnick, H., L.A. Barroso, S. Mocarquer, and B. Bezerra, 'A Delicate Balance in South America', *IEEE Power and Energy Magazine*, Vol. 6, No. 4, 2008, pp. 22–35.
- Saucedo, G., R. Perucca, and D. Kurtz, *Evolución de Las Áreas Quemadas En Corrientes Según Coberturas Vegetales.*, Instituto Nacional de Tecnología Agropecuaria, Estación Experimental Corrientes., Corrientes, 2022.
- Silvestri, G., and C. Vera, 'Nonstationary Impacts of the Southern Annular Mode on Southern Hemisphere Climate', *Journal of Climate*, Vol. 22, No. 22, November 15, 2009, pp. 6142–6148.
- Spennemann, P., G. Naumann, M. Fernández Long, M. Salvia, M. Maas, C. Cammalleri, and G. Podestá, 'Evaluación Preliminar de Un Índice Combinado de Sequías En La Pampa Húmeda de Argentina', *CONGREGMET*, Buenos Aires, 2022.
- Svoboda, M., D. LeCompte, M. Hayes, R. Heim, K. Gleason, J. Angel, B. Rippey, R. Tinker, M. Palecki, and D. Stooksbury, 'The Drought Monitor', *Bulletin of the American Meteorological Society*, Vol. 83, No. 8, 2002, pp. 1181–1190.
- Treboux, J., and E. Terré, 'En el tramo Santa Fe al Norte de la Hidrovía Paraguay-Paraná se transportaron al menos 19,1 millones de toneladas de mercadería en 2021', *Bolsa de Comercio de Rosario*, September 29, 2022. <http://www.bcr.com.ar/es/mercados/investigacion-y-desarrollo/informativo-semanal/noticias-informativo-semanal/en-el-tramo>.
- Vicente-Serrano, S.M., S. Beguería, and J.I. López-Moreno, 'A Multiscalar Drought Index Sensitive to Global Warming: The Standardized Precipitation Evapotranspiration Index', *Journal of Climate*, Vol. 23, No. 7, 2010, pp. 1696–1718.
- Vicente-Serrano, S.M., C. Gouveia, J.J. Camarero, S. Beguería, R. Trigo, J.I. López-Moreno, C. Azorín-Molina, et al., 'Response of Vegetation to Drought Time-Scales across Global Land Biomes', *Proceedings of the National Academy of Sciences*, Vol. 110, No. 1, January 2, 2013, pp. 52–57.
- Vicente-Serrano, S.M., J.I. López-Moreno, S. Beguería, J. Lorenzo-Lacruz, C. Azorin-Molina, and E. Morán-Tejeda, 'Accurate Computation of a Streamflow Drought Index', *Journal of Hydrologic Engineering*, Vol. 17, No. 2, February 1, 2012, pp. 318–332.
- Wan, Z., and Z.-L. Li, 'A Physics-Based Algorithm for Retrieving Land-Surface Emissivity and Temperature from EOS/MODIS Data', *IEEE Transactions on Geoscience and Remote Sensing*, Vol. 35, No. 4, July 1997, pp. 980–996.
- WMO, *State of the Climate in Latin America and the Caribbean 2021 (WMO-No. 1295)*, WMO, WMO, Geneva, 2022.

List of abbreviations and definitions

ANA	Agência Nacional de Águas e Saneamento Básico (Brazilian National Water and Sanitation Agency)
CEMADEN	Centro Nacional de Monitoramento e Alertas de Desastres Naturais
CHIRPS	Climate Hazards Group InfraRed Precipitation with Station
EBY	Yacyretá Binational Entity
ENSO	El Niño-Southern Oscillation
FAO	Food and Agriculture Organization of the United Nations
FAPAR	Fraction of Absorbed Photosynthetically Active Radiation
FOB	Free on Board
GRACE	Gravity Recovery and Climate Experiment
GPCC	Global Precipitation Climatology Center
GWIS	Global Wildfire Information System
HPP	Hydro Power Plant
IBAMA	Instituto Brasileiro do Meio Ambiente e dos Recursos Naturais Renováveis
INA	Instituto Nacional del Agua
INTA	Instituto Nacional de Tecnología Agropecuaria
IRI	International Research Institute for Climate and Society – Columbia Climate School
JRC	Joint Research Centre of the European Commission
MODIS	Moderate Resolution Imaging Spectroradiometer
NOAA	National Oceanic and Atmospheric Administration
ONS	Operador Nacional do Sistema Elétrico - Brazil
SISSA	Drought Information System for Southern South America (Sistema de Información Sobre Sequías para el Sur de Sudamérica)
SMN	Servicio Meteorológico Nacional – Argentina
SPI	Standardized Precipitation Index
SPEI	Standardized Precipitation-Evaporation Index
SSFI	Standardized Streamflow Index
Suomi NPP	Suomi National Polar-orbiting Partnership
TWS	Total Water Storage
UNESCO	United Nations Educational, Scientific and Cultural Organization
VIIRS	Visible Infrared Imaging Radiometer Suite
WMO	World Meteorological Organization

List of figures

Figure 1. The Paraná River near Corrientes in Argentina on 27 November 2022. Credit: European Union, Copernicus Sentinel-2 imagery.	6
Figure 2. SPI-9 from 2019 to 2022 (accumulation period from September year-1 to May of the year under analysis) based on ECMWF reanalysis ERA5. White areas indicate near-normal conditions, i.e., the index is neither very positive (indicating wet conditions) nor very negative (suggesting dry conditions). Reference baseline: 1991-2020.	9
Figure 3. Drought categories for the La Plata Basin derived from CHIRPS precipitation anomalies aggregated by 6-month periods and displayed at monthly intervals covering the period from 15 September 2021 to 15 August 2022. The dates shown in each panel correspond to the end of each 6-month period used to calculate CHIRPS precipitation totals. Source: SISSA.	10
Figure 4. Percentage of area in the La Plata Basin under each of the five drought categories used in Figure 3, from March 2019 to August 2022. The areas were derived from CHIRPS precipitation values aggregated over 6-month periods. For scale and colours, please refer to Figure 3. Source: SISSA.	11
Figure 5. Soil Moisture anomalies (with reference to 2001-2017) across parts of Southern America for the period from September 2018 to June 2022. The maps are represented at the 3 rd 10-day period of each month and computed over a 30-day period, hence almost corresponding to a regular month.	12
Figure 6. GRACE Total Water Storage Anomaly covering the period from September 2018 to June 2022 (no data is available for September 2018).	13
Figure 7. Spatial extent in percentage for FAPAR (upper panel) and Soil Moisture (lower panel) anomalies in São Paulo region. Time series cover the period from May 2021 to July 2022.	14
Figure 8. As Figure 7, but for the Mato Grosso do Sul region.	14
Figure 9. As Figure 7, but for Paraguay.	15
Figure 10. Standardized Streamflow Index (SSFI) at Corrientes, Argentina, from January 2016 to June 2022. Negative SSFI values (red bars) indicate negative streamflow anomalies. The dashed grey line shows the smoothed trend and the associated confidence interval. Source: Instituto Nacional del Agua, Argentina.	16
Figure 11. Standardized Streamflow Index (SSFI) covering the period 1981 until June 2022, at time scales of 12 months (left panel) and 24 months (right panel), for the HPP in the sub-basins of Emborcação, Furnas, Jurumirim, Foz do Areia and Itaipu. Source: CEMADEN.	17
Figure 12. Combined Drought Index (CDI) for Oct-Nov-Jan-Feb of the warm season 2021-2022. The CDI is shown on the rightmost column, while the first three columns on the left show the indicators that contribute to the index calculation: Standardized Precipitation Index (SPI-3, first column from the left), Soil Moisture Anomalies (SMA, second column), and FAPAR Anomalies (third column). Adapted from Spennemann et al., 2022.	18
Figure 13. SPI-3 (left), SMA (central), FAPAR Anomalies (right) at the end of September 2022.	19
Figure 14. La Niña seasonal ERA5 precipitation composites (mm/day) in South America based on the Niño 3.4 (ERSST) index below -0.5 in the period 1950-2022. Centre left: Mar-May, centre right: Jun-Aug, bottom left: Sep-Nov, bottom right: Dec-Feb. Top: Seasonal Niño 3.4 index (ERSST). Light shaded regions are not significant at the 90% confidence level ($p > 10\%$). Source: WMO-KNMI climate explorer https://climexp.knmi.nl	21
Figure 15. Same as Figure 14, but for the positive Antarctic Oscillation - AAO ERA5 precipitation composites (mm/day) based on CPC-NOAA index above 0.5 in the period 1979-2022. Source: WMO-KNMI climate explorer https://climexp.knmi.nl	22
Figure 16. Probabilistic precipitation forecasts for (a) SON 2021, (b) DJF 2021/2022, (c) MAM 2022, (d) JJA 2022, and e) ASO 2022, f) OND 2022 from initial conditions of August 2021, November 2021, February 2022, May 2022, July 2022 and September 2022 respectively. Forecasts were elaborated with the Copernicus Climate Change Service (C3S) multi-model system. Precipitation categories are defined by the terciles of the distribution (below normal, near normal and above normal). The figure shows only the most likely category for each grid point. Thus, brown colours denote highest chances for below normal precipitation, while green values correspond to higher chances for above normal precipitation. White colours indicate higher chances for precipitation near normal or equal probabilities for the terciles. Source: Copernicus Climate Change Service().	24

Figure 17. (a) Niño 3.4 index, calculated as the area-averaged sea surface temperature anomalies (°C) at 5N-5S, 170W-120W. Source: NOAA, CPC(), (b) Monthly evolution of the Southern Oscillation Index defined as the standardized sea-level pressure anomaly (hPa) differences between Tahiti and Darwin (SOI, dots) and five-month running mean (lines). Source NOAA, CPC(). Data from 2003 updated through August 2022.	24
Figure 18. Upper panel: Time series of predicted sea surface temperature anomalies for the Niño 3.4 region (in degrees C) from various dynamical and statistical models for nine overlapping 3-month periods from ASO 2022 to MJJ 2023. Lower panel: Time series of predicted sea surface temperature anomalies for the Indian Ocean Dipole region (in degrees C) from various dynamical models for seven months. Source: International Research Institute for Climate and Society (IRI)() and APEC Climate Center()	25
Figure 19. Upper Panel: Annual mean Pacific Decadal Oscillation - PDO (left) and Atlantic Multidecadal Oscillation – AMO (right) indices (Extended Reconstructed Sea Surface Temperature, ERSST). Lower Panel: Annual ERA5 precipitation composites (mm/day) in South America for PDO values below -0.5 (left) and AMO values over 0.1 (right). Period of analysis 1950-2021. Source: WMO-KNMI climate explorer https://climexp.knmi.nl	26
Figure 20. Left: WMO multi-system mean precipitation predictions for 2022-2026 in models initialized in 2021. Top right: WMO multi-system mean (red line), spread (shading) predicted PDO index in models initialized in 2021. Bottom right: WMO multi-system mean (red line), spread (shading) predicted AMO index in models initialized in 2021. Black lines represent the observed values. Source: https://hadleyserver.metoffice.gov.uk/wmolc/	27
Figure 21. Time series of SPEI-3 values at a meteorological station operated by Argentine agricultural research institute (INTA) near Mercedes, Corrientes. The sharp decrease during February 2022 (shaded area) is well visible. Note that SPEI-3 values lower than -3.00 are truncated for display purposes. Source: SISSA.	29
Figure 22. Evaporative Stress Index (ESI) percentiles for the 4-week period ending on 29 January 2022. The white bold line indicates the Province of Corrientes, and the red dot denotes the location of the Mercedes INTA meteorological station for which SPEI-3 values were shown in Figure 21. Source: SISSA.	30
Figure 23. Areas burned in the Province of Corrientes, Argentina by 27 February 2022. Source: INTA Corrientes (see Saucedo et al. 2022).	31
Figure 24. The consequences of dry conditions in the Pampas plains near the city of Buenos Aires (upper right corner of each image) are visible when comparing these two images acquired by Copernicus Sentinel-2 in September 2018 (above) and September 2022 (below). Source: European Union, Copernicus Sentinel-2 imagery.	33
Figure 25. Anomalies (in cm) of the Upper Paraguay River level at Ladário. Base period is 1900-2020. Source: CEMADEN	34
Figure 26. Hydrometric level of the Paraná River at the City of Rosario, Argentina, January 2016 to June 2022. The dashed red line indicates monthly median heights (calculated using the base period 1989-2020). Source: Instituto Nacional del Agua, Argentina.	35
Figure 27. Monthly hydropower generation for the previous 12 months. Source: websites of the national transmission system operators for countries shown (data updated 01/10/2022 – see footnotes at page 36). ..	37
Figure 28. Example of a drought status report produced by Argentine Drought Monitoring Roundtable, July 2022. The map in the report shows moderate drought in the Pampas of central-eastern Argentina. Source: Mesa Nacional de Monitoreo de Sequías, Argentina().	38
Figure 29. Brazilian Drought Monitor map for July 2022. In the Southeast Region, due to negative rainfall anomalies and worsening indicators, there was an increase in the area with weak drought (S0) in the north of Minas Gerais and Rio de Janeiro. Drought worsened in the states of Espírito Santo and east-central Minas Gerais, going from weak (S0) to moderate (S1) conditions. Source: https://monitordesecas.ana.gov.br	39
Figure 30. Integrated drought index for July 2022 considering the 6-month temporal scale indicating drought severity over Brazilian municipalities. Source: CEMADEN.	40
Figure 31. Using agricultural drought indicators filtered by an agricultural land mask, CEMADEN estimates the percentage of agricultural area at the municipality level affected by drought. It is also possible to have a	

diagnosis of the sizes of the most affected rural establishments. The figure shows the conditions for August 2022. Source: CEMADEN. 41

Figure 32. Example of drought monitoring and projections of the Cantareira system, the largest water supply system for the Metropolitan Region of São Paulo. Upper left: SPI values at time scales of 6 to 36 months show the long-term drought conditions for July 2022. Upper right: time series of SSFI at 12-time and 36-time scale show the critical hydrological situation (hydrological drought) since 2014. Lower left and right: The projected inflow and reservoir level obtained from hydrological modelling. Source: CEMADEN. 42

Figure 33. Time series of the areas under different drought conditions in two regions in the eastern part of Bolivia that are part of the La Plata Basin: Chiquitania (above) and Chaco (below); see the inset map on the left for the location of these regions. An increase in the areas under weak (S1) and moderate (S2) drought conditions can be seen starting in mid-2021. Source: Bolivian Drought Monitor (<http://monitoresequias.senamhi.gob.bo>) 43

Figure 34. Left: INUMET SPI-3 map for Uruguay, September 2022 derived from data at 18 in-situ meteorological stations. Centre: Soil water balance (INIA/GRAS and INUMET) for the third decade of December 2021, showing country-wide moisture deficits. Right: NDVI anomalies in December 2021 produced by INIA/GRAS..... 44

List of tables

Table 1. Hydropower generation and share of total electrical generation in 2020. Source: International Renewable Energy Agency, IRENA, Statistical Profiles, <https://www.irena.org/Statistics/Statistical-Profiles>. 36

Annexes

Annex 1. Description of drought indicators used in this report

This annex contains a non-exhaustive list and a brief description of the main drought indicators used in this report. The monitoring of droughts is based on the analysis of a series of indicators, representing different components of the hydrological cycle (e.g., precipitation, soil moisture, reservoir levels, river flow, groundwater levels) or specific impacts (e.g., vegetation water stress) that are associated with a particular type of drought.

For further information please refer to the factsheets section of the European and Global Drought Observatory ⁽¹⁷⁾, ⁽¹⁸⁾. The Global Drought Observatory (GDO) is a service run by the European Commission's Joint Research Centre. The GDO portal contains drought information, graphs, and time-series at Global level. All drought indicators can now be accessed for public download from the dedicated page on the GDO ⁽¹⁹⁾.

Standardized Precipitation Index (SPI)

The ongoing drought episode over La Plata Basin is characterised and described starting with the analysis of precipitation patterns focusing on Standardized Precipitation Index (SPI). SPI is one of the most used and common indicators for drought analysis and evaluation. This statistical index measures precipitation anomalies comparing the total precipitation received at a particular location during a period of n months with the long-term precipitation distribution for the same period of time at that location. Monthly accumulation periods (n) are 1, 3, 6, 9, 12, 24 or 48 months. In this report the corresponding SPIs are denoted as SPI-1, SPI-3, SPI-6 and SPI-12 and the reference period is 1991-2020.

Each accumulation period describes a different aspect of the drought and its potential impacts. SPIs for short accumulation periods (e.g., SPI-1 to SPI-3) are indicators for immediate impacts such as reduced soil moisture, snowpack, and flow in smaller creeks. SPIs for medium accumulation periods (e.g., SPI-3 to SPI-12) are indicators for reduced stream flow and reservoir storage. SPIs for long accumulation periods (SPI-12 to SPI-48) are indicators for reduced reservoir and groundwater recharge, for example. The exact relationship between accumulation period and impact depends on the natural environment (e.g., geology, soils) and the human interference (e.g., existence of irrigation schemes). More details in *(McKee, Doesken, and Kleist, 1993)*

Soil Moisture Anomalies

Soil moisture anomalies are computed on a 30-day moving window at a spatial resolution of 0.1 decimal degrees and updated every 10 days. The index is computed as a weighted average of three standardized variables: 1) LISFLOOD root zone soil moisture, 2) MODIS Land Surface Temperature, and 3) ESA CCI remote sensing skin soil moisture. All three variables are standardized on the same baseline period 2001-2016 and the weighting factors are computed as described in *(Cammalleri et al., 2017)*. The full ensemble of the three models is provided up to the second-to-last 10-days period, whereas the last 10-days period is a 'first-guess' estimate based only on LISFLOOD and MODIS LST data.

GRACE Total Water Storage anomaly

The Total Water Storage (TWS) anomaly is computed as standardized deviation of the GRACE satellite Liquid Water Equivalent (JPL TELLUS, Level 3 release 6.0, <https://grace.jpl.nasa.gov/>) from the baseline 2002-2017. The dataset is monthly at 1-degree resolution. Details on the relationship between this indicator and classic meteorological drought indices (e.g., SPI) can be found in *(Cammalleri, Barbosa, and Vogt, 2019)*.

⁽¹⁷⁾ <https://edo.jrc.ec.europa.eu/edov2/php/index.php?id=1101>

⁽¹⁸⁾ <https://edo.jrc.ec.europa.eu/gdo/php/index.php?id=2101>

⁽¹⁹⁾ <https://edo.jrc.ec.europa.eu/gdo/php/index.php?id=2112>

Fraction of Absorbed Photosynthetically Active Radiation (FAPAR)

The FAPAR Anomaly indicator that is implemented in the Copernicus Global Drought Observatory (GDO) is used to detect and monitor the impacts on vegetation growth and productivity of environmental stress factors, especially plant water stress due to drought. The FAPAR Anomaly indicator is computed as deviations of the satellite-measured biophysical variable Fraction of Absorbed Photosynthetically Active Radiation (FAPAR, sometimes written as fAPAR or FPAR), composited for 10-day intervals, from its long-term mean values. FAPAR is one of the 50 so-called “Essential Climate Variables” (ECVs) that have been defined by the Global Climate Observing System as being both feasible for global climate observation, and important to support the work of the United Nations Framework Convention on Climate Change and the Intergovernmental Panel on Climate Change. (Of the 50 ECVs, 26 are listed as being significantly dependent on satellite observations). FAPAR values and their anomalies have been shown to be good indicators for detecting and assessing drought impacts on plant canopies, such as agricultural crops and natural vegetation, and thus provide information that is potentially useful for water and agricultural management purposes. More details can be found in (Gobron et al., 2005).

Low Flow Index

The Low-Flow Index (LFI) indicator, is used for the operational, near real-time monitoring of hydrological (i.e. streamflow) drought in Europe. At global level the LFI is an experimental product. The LFI indicator exploits the simulated daily river water discharge outputs of the LISFLOOD hydrological model, in order to capture unbroken consecutive periods of unusually low streamflow, and compares the consequent water deficit during those periods with the historical climatological conditions, in order to derive the severity of the events. A key advantage of the LFI indicator, compared for instance with the widely used Standardized Runoff Index (SRI), is that the LFI indicator directly exploits daily streamflow values, allowing a near real-time update of the index at regular time steps. More information can be found in (Cammalleri, Vogt, and Salamon, 2017; Cammalleri, Barbosa, and Vogt, 2020).

Risk of Drought Impacts for Agriculture (RDRI-Agri)

The Risk of Drought Impacts for Agriculture (RDRI-Agri) indicator that is implemented in the Global Drought Observatory is used for determining the area more likely to be affected by droughts. The RDRI-Agri indicator is computed as the combination of the dynamic layers of drought hazard, exposure and vulnerability. Higher risk means that the areas affected will be the most likely to report impacts due to droughts.

Maps of RDRI-Agri provide information on the spatial distribution of the risk of drought impacts globally, and their evolution over time. The maps of the RDRI-Agri indicator can be used as a proxy for the presence of potential impacts due to ongoing droughts. Due to the complexity of drought propagation through the hydrological cycle and different socio-economic sectors, as well as cascading effects, these impacts may well be observed much later. More information can be found in (Carrao, Naumann, and Barbosa, 2016)

GETTING IN TOUCH WITH THE EU

In person

All over the European Union there are hundreds of Europe Direct centres. You can find the address of the centre nearest you online (european-union.europa.eu/contact-eu/meet-us_en).

On the phone or in writing

Europe Direct is a service that answers your questions about the European Union. You can contact this service:

- by freephone: 00 800 6 7 8 9 10 11 (certain operators may charge for these calls),
- at the following standard number: +32 22999696,
- via the following form: european-union.europa.eu/contact-eu/write-us_en.

FINDING INFORMATION ABOUT THE EU

Online

Information about the European Union in all the official languages of the EU is available on the Europa website (european-union.europa.eu).

EU publications

You can view or order EU publications at op.europa.eu/en/publications. Multiple copies of free publications can be obtained by contacting Europe Direct or your local documentation centre (european-union.europa.eu/contact-eu/meet-us_en).

EU law and related documents

For access to legal information from the EU, including all EU law since 1951 in all the official language versions, go to EUR-Lex (eur-lex.europa.eu).

Open data from the EU

The portal data.europa.eu provides access to open datasets from the EU institutions, bodies and agencies. These can be downloaded and reused for free, for both commercial and non-commercial purposes. The portal also provides access to a wealth of datasets from European countries.

The European Commission's science and knowledge service

Joint Research Centre

JRC Mission

As the science and knowledge service of the European Commission, the Joint Research Centre's mission is to support EU policies with independent evidence throughout the whole policy cycle.



EU Science Hub
joint-research-centre.ec.europa.eu



@EU_ScienceHub



EU Science Hub - Joint Research Centre



EU Science, Research and Innovation



EU Science Hub



EU Science



Publications Office
of the European Union